Duo pack EDT2 IGBT and EmCon3 diode in TO247 Plus package

Product description, electrical and thermal specifications

About this document

Scope and purpose

This application note shows implementation hints and benefits for AIKQ120N75CP2 and AIKQ200N75CP2 devices in traction inverters. This document is intended to give a deeper and comprehensive look at the way these two products can be integrated into an automotive traction drive system. It also provides hints and examples on some of the scenarios that a system developer might encounter while studying the switching, short circuit, paralleling, and thermal behavior of the system.

Intended audience

This application note is intended for engineers evaluating the implementation of AIKQ200N75CP2 and AIKQ120N75CP2 products. The main focus is to provide hints in the design and implementation of inverters for automotive applications. A moderate level of knowledge in electrical and thermal design is required.

Table of contents

1 Product description

AIKQ200N75CP2 and AIKQ120N75CP2 products are discrete EDT2 IGBTs with co-packed emitter-controlled third-generation diodes in TO-247-3 package, designed for discrete main inverter systems.

The EDT2 IGBT technology has an automotive Micro-Pattern Trench-Field-Stop cell design. This technology is already successfully used in several automotive inverter modules like EasyPACK™ 2B EDT2 or HybridPACK™ (FS650R08A4P2). Generally, EDT2 chips have a maximum breakdown voltage of 750 V, enabling DC bus systems to operate up to 470 V and providing a higher margin for voltage overshoots. In the example of Chapter 3.5.3, a 470 V system is compared with a 400 V system using both devices. When operating an AIKQ120N75CP2 at 470 V V_{dc}, the total power output increases in 11%, and the efficiency of the system increases around 0.3%.

Moreover, EDT2 technology has a tight parameter distribution and a positive thermal coefficient. For example, V_{ce} sat difference between typical and maximum values is less than 100 mV[1)], and V_{GEth} difference is less than 750 mV. This enables easy paralleling operation, providing system flexibility and power scalability to the final designs.

The AIKQ200N75CP2 classifies as the best in class discrete IGBT in a TO247 Plus package since it has the highest nominal current-carrying capability in the market. I_{c_nom} is 200 A at T_c = 100°C without bond-wire limitation. This feature reduces the number of paralleled devices required to reach a certain power class, increasing power density and reducing the overall system cost.

AIKQ120N75CP2 is a successor product for Infineon's previous generation of traction inverter IGBT devices such as the AUIRGPS4070D0 and AIKQ120N60CT. In addition, it is a drop-in replacement for competitors' 120 A nominal current devices (at T_c = 100°C), bringing the unique efficiency of the EDT2 technology to existing systems. In the example explored in Chapter 3.5.1, the total system efficiency increases by 1% when replacing a 160 A competitor's device. Also, the heatsink R_{th} requirement becomes less demanding, changing from 0.5 K/W with the competitor device to 0.73 K/W with the AIKQ120N75CP2. Reduction of system cost due to efficiency can be therefore be achieved with these device families. Also, in Chapter 3.5.2, a power output increase of 23% and 4% is calculated when replacing the competitor device and the previous generation, respectively.

The nominal currents of these devices are 120 A and 200 A and both have very low forward voltages of 1.3. In the 120 A class, the EDT2 device has 13% less V_{ce} sat at nominal conditions compared with the previous generation AIKQ120N60CT. Conduction losses at nominal value are therefore reduced by 13%. This device family is short circuit robust and has a withstand time of up to 5 us at nominal conditions.

The co-packed diodes are fast recovery anti-parallel emitter-controlled third-generation chips. This pair was selected due to its efficient and soft switching behavior. As an example, the total switching losses in the AIKQ120N75CP2 at 120 A, 400 V, T_j = 175°C with R_g = 3 Ω are 10% less compared to the AIKQ120N60CT. E_{ts} = 9.1 mJ for the EDT2 and E_{ts} = 10.01 mJ for the previous AIKQ120N60CT at this condition.

Infineon's AIKQ200N75CP2 and AIKQ120N75CP2 package (shown in Figure 1), two groves can be identified on the package, increasing the creep-age distance to more than 4 mm for higher pollution degree environments as well as increasing voltage operation.

In the next section, the key features and overall benefits are listed.

1 Measured at I_C = 200.0 A, V_{GE} = 15 V, T_{vj} = 25°C.

1 Product description

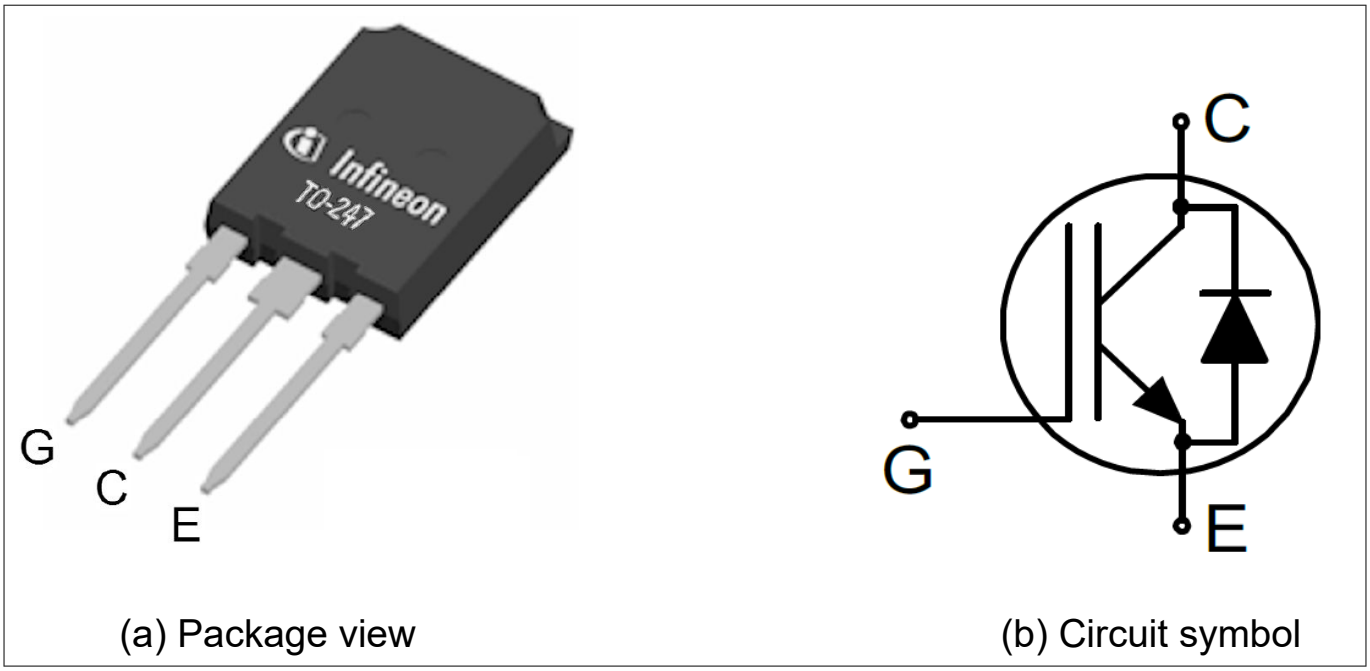

Figure 1 **Infineon's AIKQ200N75CP2 and AIKQ120N75CP2**

Table 1 **Key performance and package parameters**

Type	V_{CE}	I_C, T_c = 100°C	V_{CEsat}, T_{vj} = 25°C	T_{vjmax}	Marking	Package
AIKQ200N75CP2	750 V	200 A	1.3 V	175°C	AKQ20FCP	PG-TO247-3-46
AIKQ120N75CP2	750 V	120 A	1.3 V	175°C	AKQ12FCP	PG-TO247-3-46

1.1 EDT2 technology offering

- 750 V collector-emitter blocking voltage capability
- Suitable for 470 V V_{dc} systems and increase overvoltage margin for 400 V V_{dc} systems
- Very low $V_{CE(sat)}$ = 1.30 V (typical)
- Short circuit robust
- T_{sc} = 5 us at V_{CE} = 470 V, V_{GE} = 15 V
- Self-limiting current under short circuit condition
- Positive thermal coefficient and very tight parameter distribution for easy paralleling
- Excellent current sharing in parallel operation
- Smooth switching characteristics
- Low gate charge Q_G
- Simple gate drive design
- Co-packed with fast soft recovery emitter controlled 3 diodes
- Low EMI signature

1.2 TO-247-3-46 package

- TO247 Plus package with high creepage distance
- Compact molded Pb-free package
- High mechanical robustness
- Lead trousers to increase the creepage distance

1.3 System offering

- A reduced number of parallel devices is required due to I_{nom} = 200 A
- Drop-in replacement for previous generation devices I_c = 120 A, T_c = 100°C
- AEC-Q101 automotive qualified
- High reliability and operating lifetime

2 Thermal specification

2.1 Thermal characterization

Figure 2 illustrates the assembly for the device thermal characterization. The thermal resistance and impedance from junction to case ($R_{th(j-c)}$ and $Z_{th(j-c)}$) are key parameters to determine the thermal response of semiconductor power devices. Please note that in an actual application, the thermal resistance and impedance from case to ambient ($R_{th(c-a)}$ and $Z_{th(c-a)}$) play the most important role in thermal behavior. Therefore, a careful design of the thermal interface material and heatsink is necessary to achieve high performance of the devices.

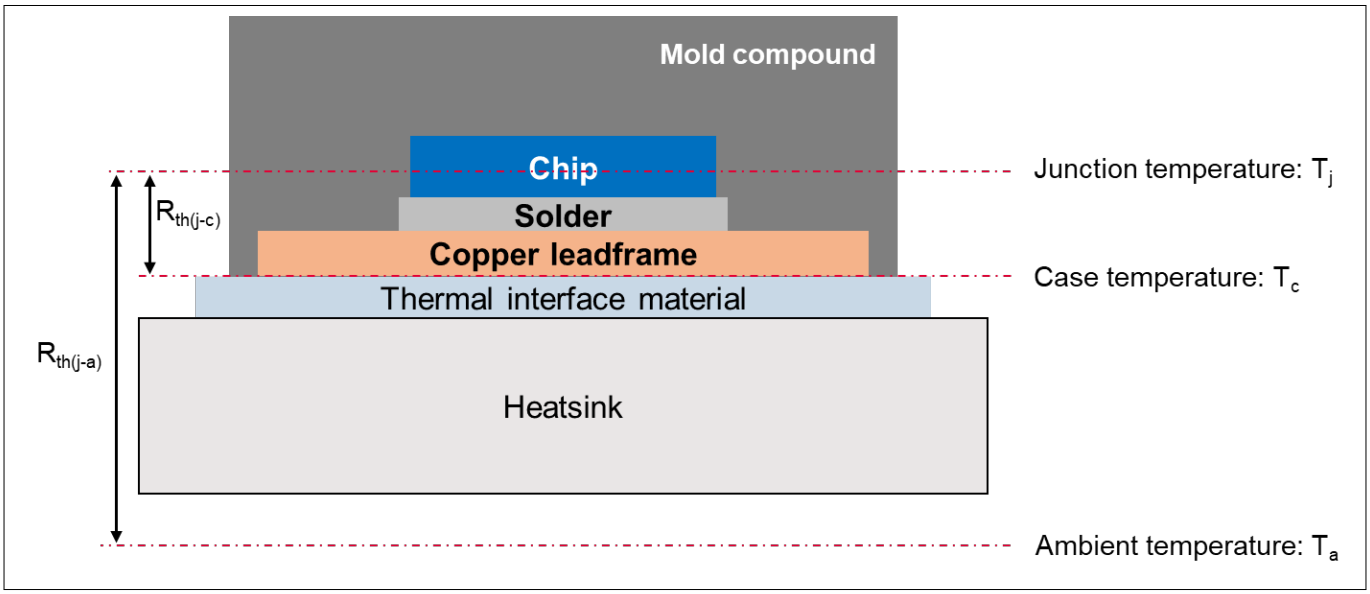

Figure 2 Thermal characterization of AIKQ200N75CP2

2.2 Transient thermal impedance of AIKQ200N75CP2

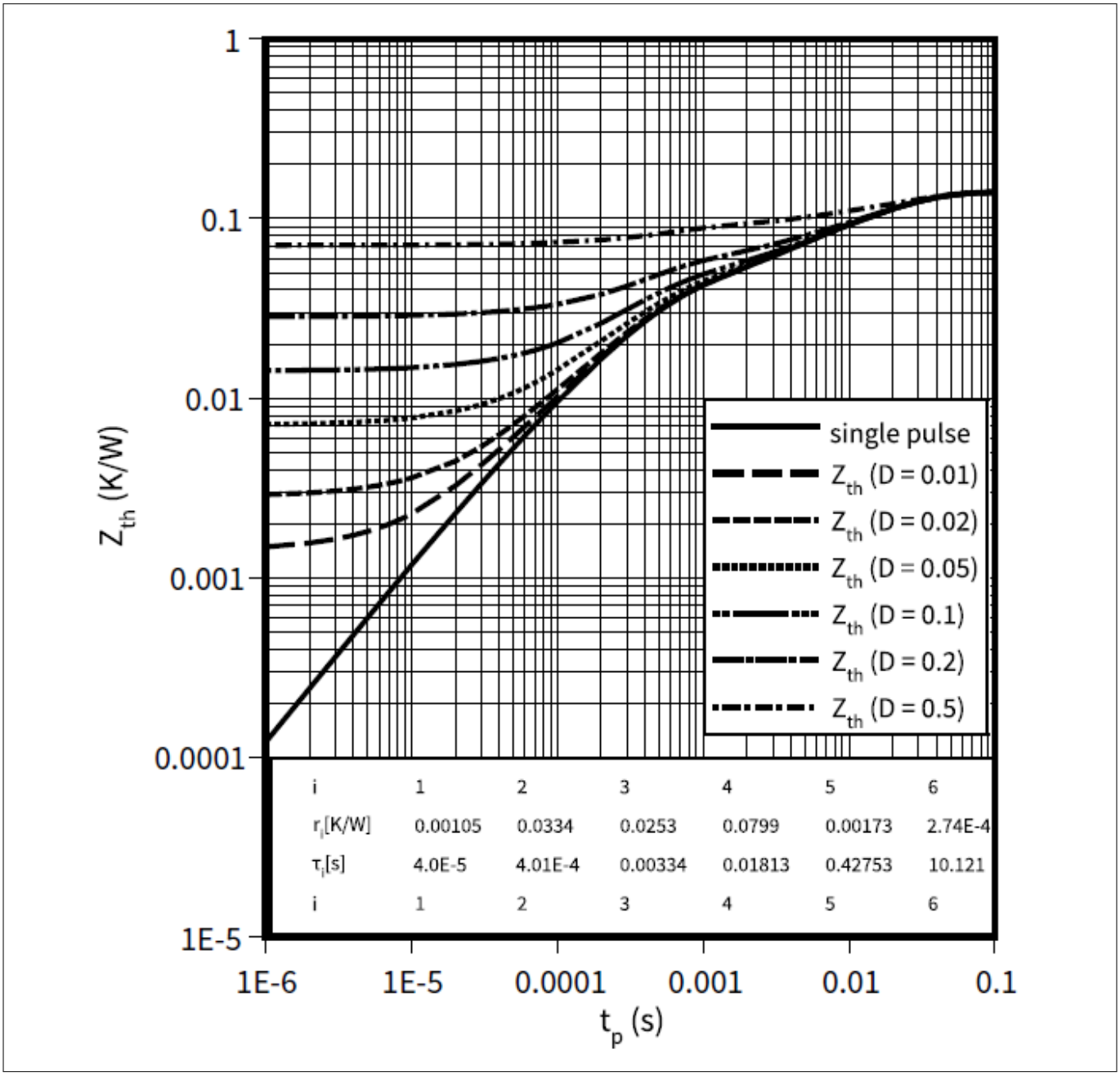

Figure 3 Transient thermal impedance junction to case of AIKQ200N75CP2 IGBT

The thermal impedance junction to case curve of AIKQ200N75CP2 IGBT obtained from thermal characterization is shown in Figure 3. The steady-state thermal resistance junction to case $R_{th(j\text{-}c)}$ is 0.14 K/W. EDT2 technology provides safe 175°C junction temperature operation. Because of the low $R_{th(j\text{-}c)}$ and high operation junction temperature, AIKQ200N75CP2 is capable of carrying 200 A DC when the case temperature is lower than 100°C. This is without any bond wire limitation. A mounting recommendation is provided down below.

Figure 4 shows the transient thermal impedance, Z_{th} curves obtained from the thermal characterization of the diode. The steady-state thermal resistance junction to case is 0.26 K/W.

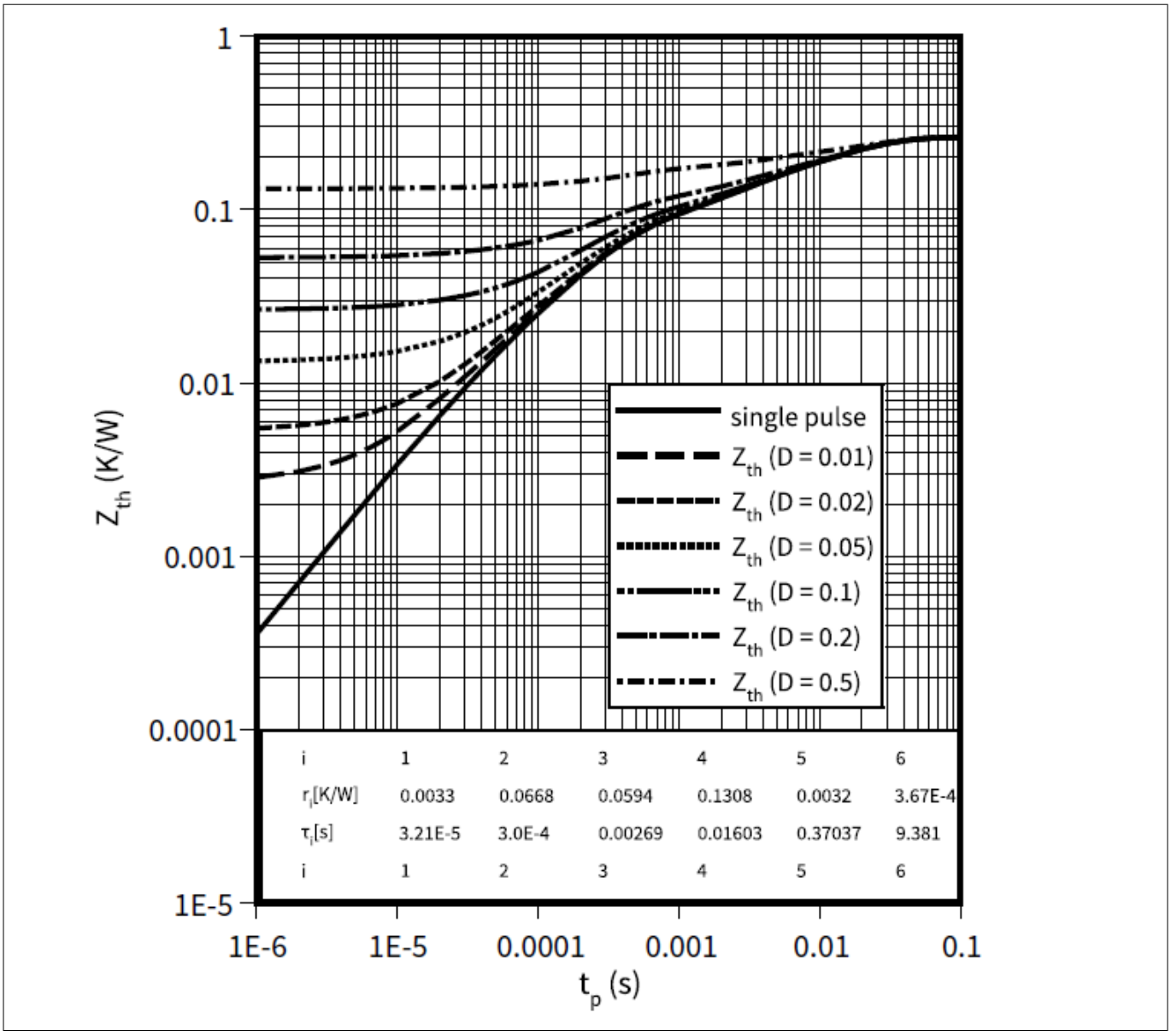

i	1	2	3	4	5	6
r_i[K/W]	0.0033	0.0668	0.0594	0.1308	0.0032	3.67E-4
τ_i[s]	3.21E-5	3.0E-4	0.00269	0.01603	0.37037	9.381
i	1	2	3	4	5	6

Figure 4 Transient thermal impedance junction to case of AIKQ200N75CP2 diode

2.2.1 PCB mounting recommendation for AIKQ200N75CP2

The AIKQ200N75CP2 provides the ability to pass 200 A through its 2 mm leads. The lead's maximum temperature of 220°C should not be exceeded during operation. To maintain the lead temperature under this range, a 4.3 mm distance from the package to the PCB is recommended. This distance is marked with the designator L1 in the package drawing. In addition, the package has a wider section for easy assembly. A mounting line is provided in Figure 5 as a reference.

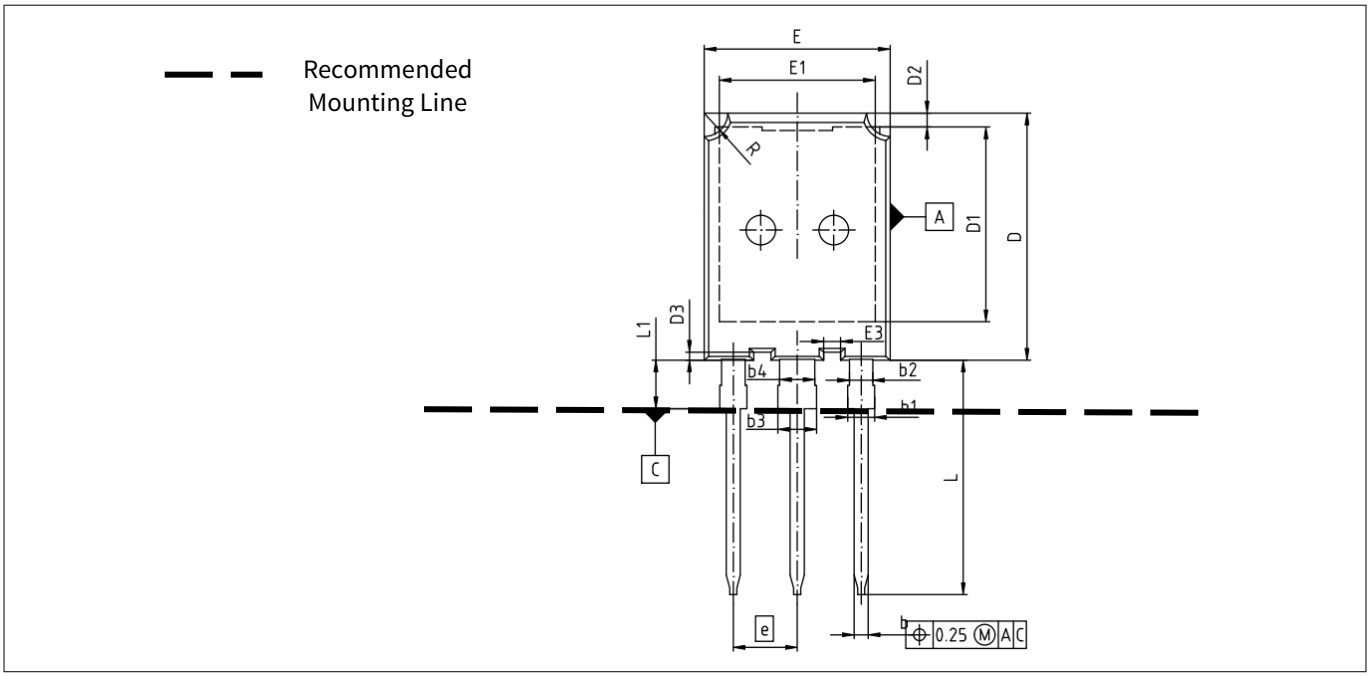

Figure 5 Package recommended mounting position

L1 corresponds to the ideal mounting distance for the package, a line shows the recommended mounting line on the PCB.

To further understand the TO247 Plus package and its assembly guidelines, please refer to AN2017-01 [1]. In the installation of these packages it is also recommended to take a special look at the electrical safety and insulation, please refer to AN 2012-10 [2].

2.3 Transient thermal impedance of AIKQ120N75CP2

Figure 6 illustrates the transient thermal impedance, junction to case of AIKQ120N75CP2 IGBT. The steady-state thermal resistance is 0.22 K/W, which is higher than that of AIKQ200N75CP2 because of the smaller chip size. With the junction temperature limited at 175°C, the device's maximum collector DC is 120 A when case temperature is 100°C.

The transient thermal impedance junction to case of the AIKQ120N75CP2 diode is shown in Figure 7. The steady-state thermal resistance is 0.40 K/W.

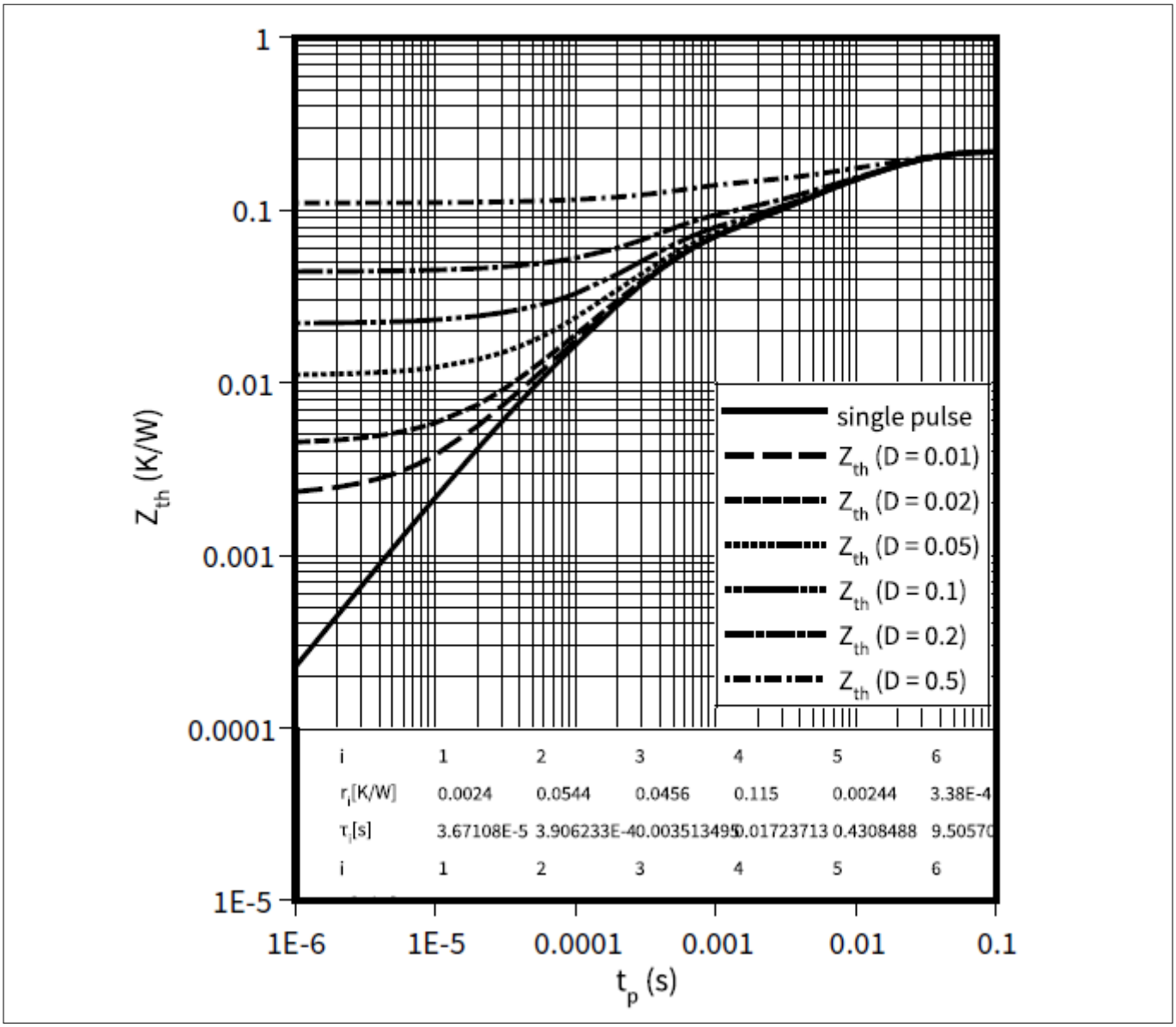

Figure 6 **Transient thermal impedance junction to case of AIKQ120N75CP2 IGBT**

2 Thermal specification

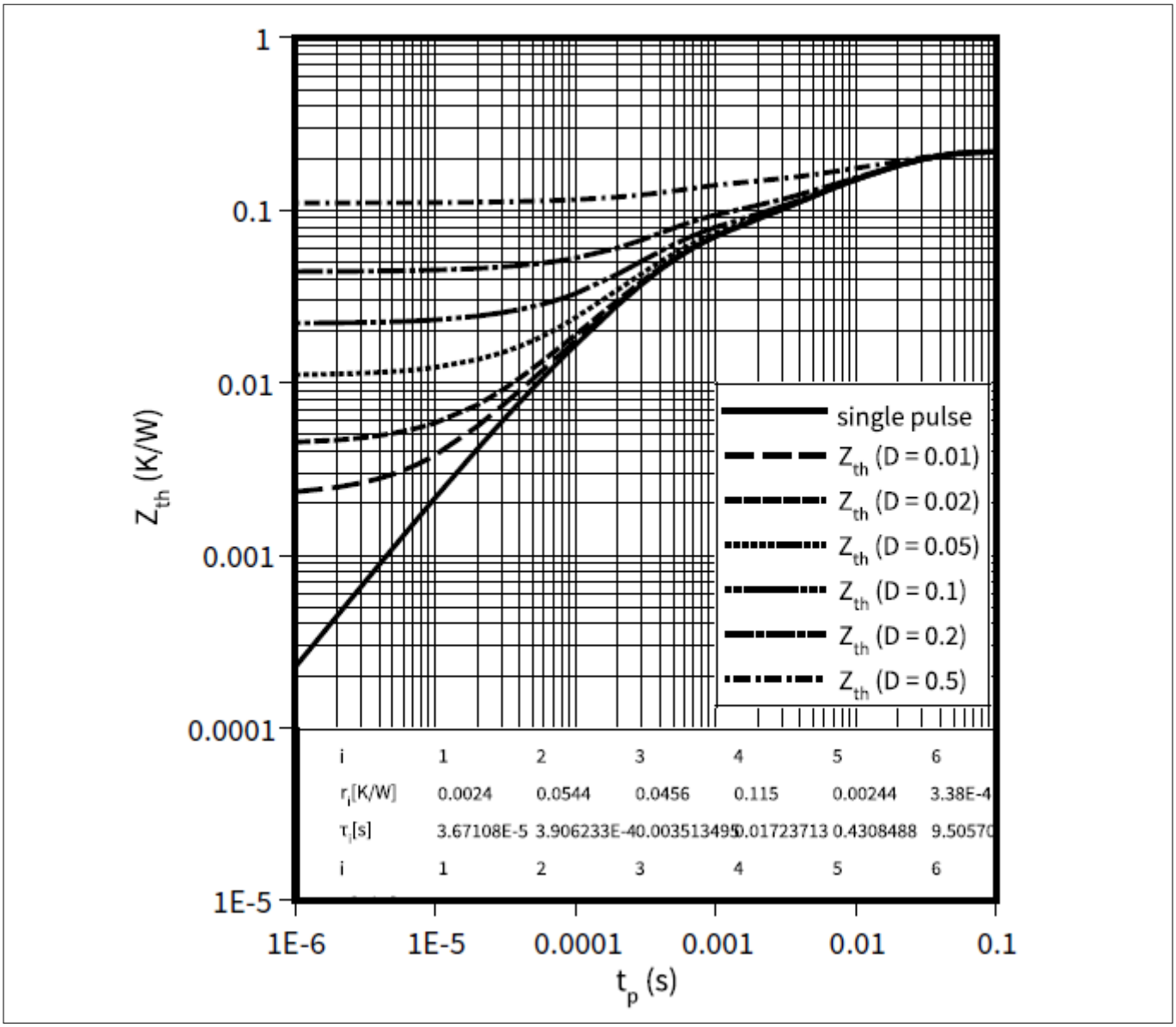

Figure 7 **Transient thermal impedance junction to case of AIKQ120N75CP2 diode**

3 Electrical specification

3.1 Static characteristics

The key static parameters of AIKQ200N75CP2:

- Collector-emitter voltage V_{CE} = 750 V
- Gate-emitter voltage V_{GE} = ±20 V
- Typical collector-emitter saturation voltage (I_C = 200 A, V_{GE} = 15 V, and T_{vj} = 25°C) $V_{CE\text{-}sat}$ = 1.30 V

The key static parameters of AIKQ120N75CP2:

- Collector-emitter voltage V_{CE} = 750 V
- Gate-emitter voltage V_{GE} = ±20 V
- Typical collector-emitter saturation voltage (I_C = 120 A, V_{GE} = 15 V, and T_{vj} = 25°C) $V_{CE\text{-}sat}$ = 1.30 V

In the datasheet, the maximum collector DC of AIKQ200N75CP2 is 200 A when the case temperature is lower than 100°C, and the maximum collector DC of AIKQ120N75CP2 is 120 A when case temperature is lower than 100°C. The DC capabilities of AIKQ200N75CP2 and AIKQ120N75CP2 are limited by bond-wire and maximum junction temperature. The curves of collector current as a function of case temperature are shown in Figure 8.

Figure 8(a) shows the collector DC limitation of AIKQ200N75CP2. The flat part of the curve (when case temperature is lower than 125°C) is limited by the bond-wire current capability, and the corresponding maximum DC is 200 A. When the case temperature is higher than 125°C, the DC is no longer limited by the bond-wire. Instead, the maximum junction temperature dominates the curve shape and should be lower than 175°C. In this region, the allowed power dissipation $P = \Delta T/R_{th}$, where $\Delta T = T_j - T_{case}$ is the temperature difference between junction and case. R_{th} is the thermal resistance from junction to case. The power dissipation P is the product of collector current and collect-emitter voltage $I_C \times V_{CE}$, and V_{CE} is a function of collector current ($V_{CE} = f(I_C)$). Therefore, by solving the equation $I_C \times f(I_C) = (T_j - T_{case})/R_{th}$, the relationship between I_C and T_{case} can be derived when case temperature is higher than 125°C.

Similarly, Figure 8(b) shows the collector DC limitation of AIKQ120N75CP2. The DC is limited by the bond-wire when the case temperature is lower than 115°C. The same method is applied to derive the curve when the case temperature is higher than 115°C.

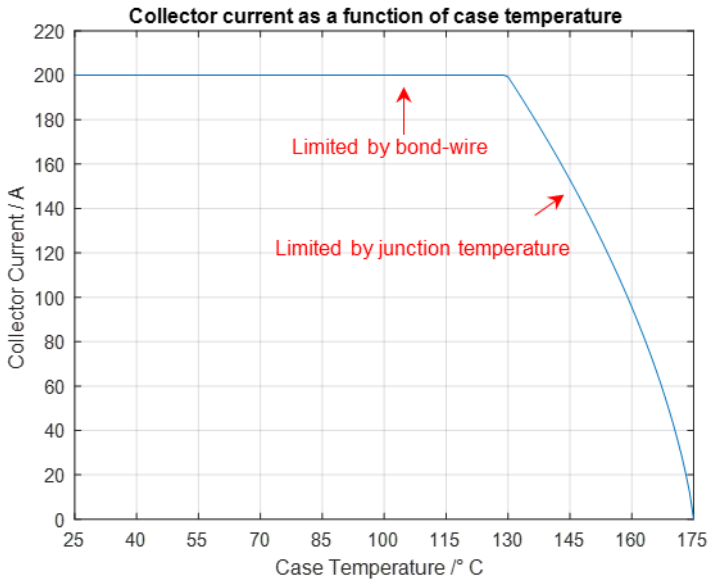

(a) DC limitation of AIKQ200N75CP2

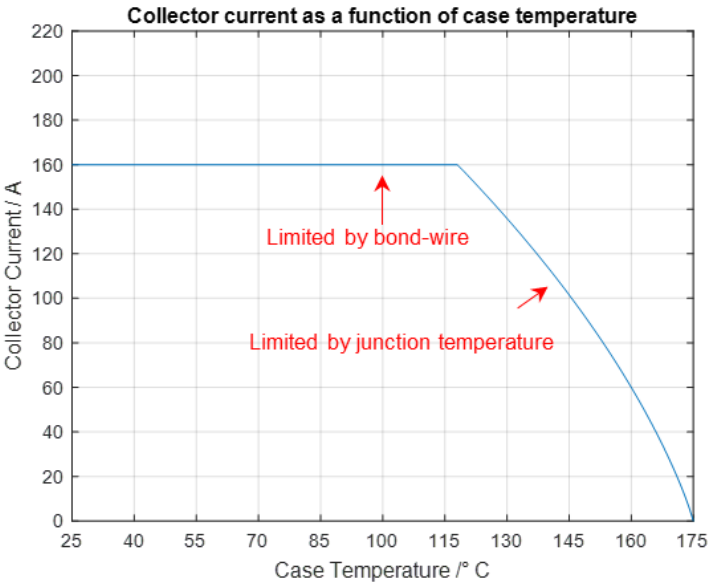

(b) DC limitation of AIKQ120N75CP2

Figure 8 Collector current as a function of case temperature

3.2 IGBT and diode switching behavior characterization

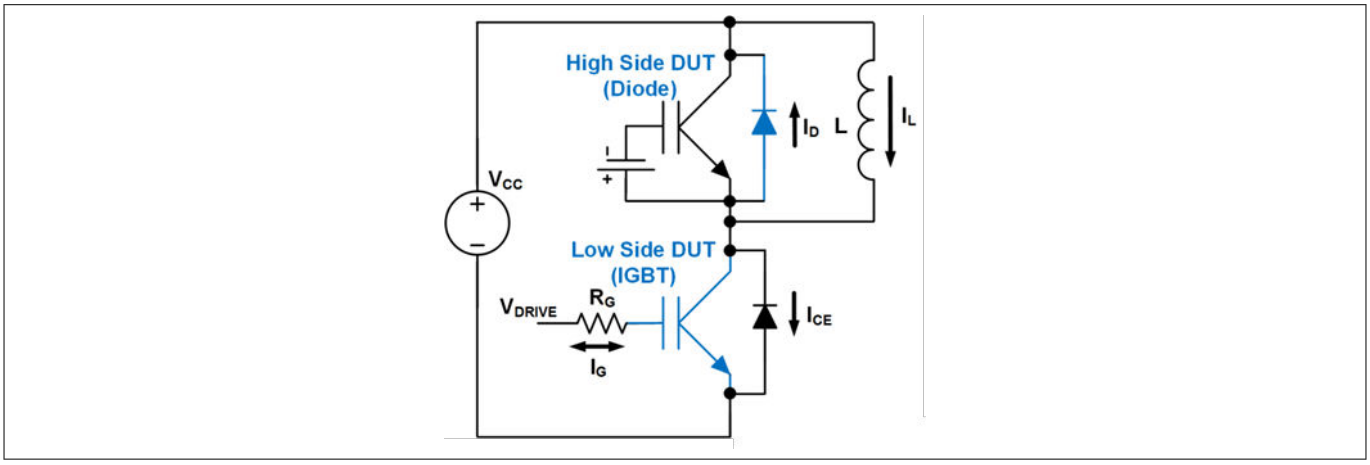

Figure 9 Methodology for switching behavior characterization of IGBT and diode

The switching performance of the IGBT and diode of AIKQ200N75CP2 and AIKQ120N75CP2 is evaluated using the schematic shown in Figure 9. In this double pulse test setup, the device under test (DUT) is the low-side IGBT and the high-side diode.

Figure 10(a) shows the turn-on transient and Figure 10(b) shows the turn-off switching behavior of AIKQ200N75CP2 IGBT at 25°C for a 200 A load current at a bus voltage of 470 V. The gate is driven from +15 V to -8 V with the gate resistance of R_G = 5 Ω. The turn-on loss is 20.42 mJ. During turn-on transient, the collector current rate-of-change d*i*/d*t* is 0.7 A/ns and the collector-emitter voltage rate-of-change is 4.1 V/ns. The turn-off loss is 8.16 mJ. During the turn-off period, the collector current rate-of-change d*i*/d*t* is 4.3 A/ns and the collector-emitter voltage rate-of-change d*v*/d*t* is 8.8 V/ns. The turn-off voltage overshoot peaks at approximately 680 V.

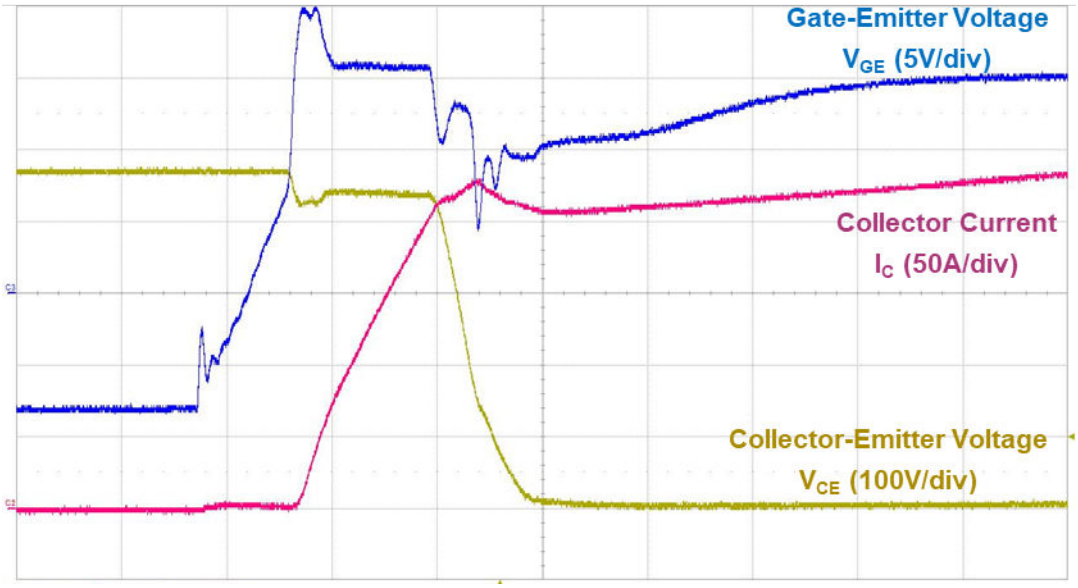

(a) Turn-on transient

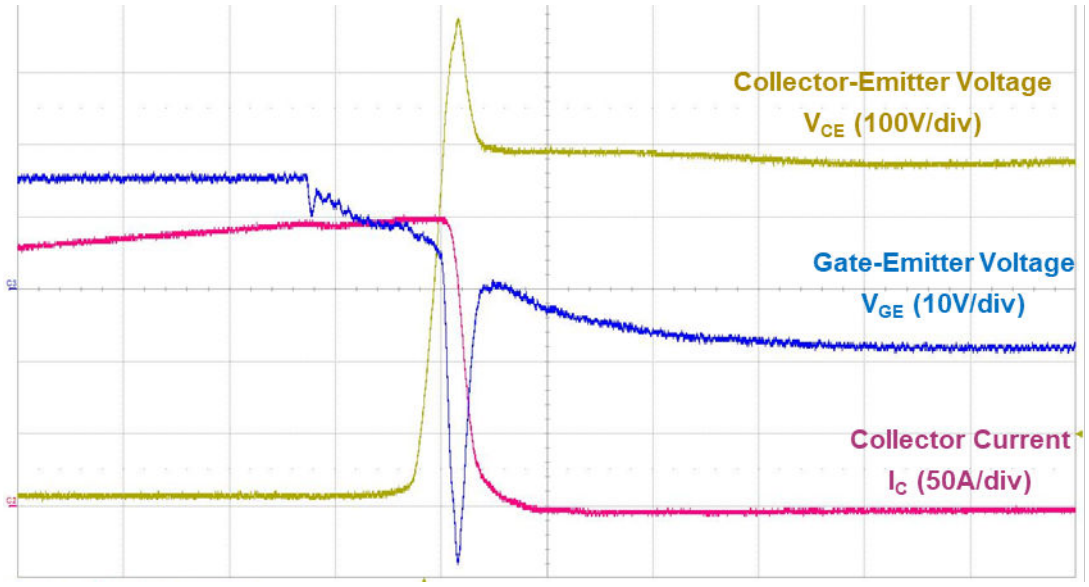

(b) Turn-off transient

Figure 10 25°C switching waveforms for AIKQ200N75CP2 IGBT at 200 A and 470 V

Figure 11 shows the high side diode's reverse recovery behavior during turn-on of the low side IGBT at 25°C. The peak reverse recovery current I_{rrm} is approximately 41 A. The reverse recovery charge is 4.7 µC and the energy loss is 1.49 mJ at 25°C.

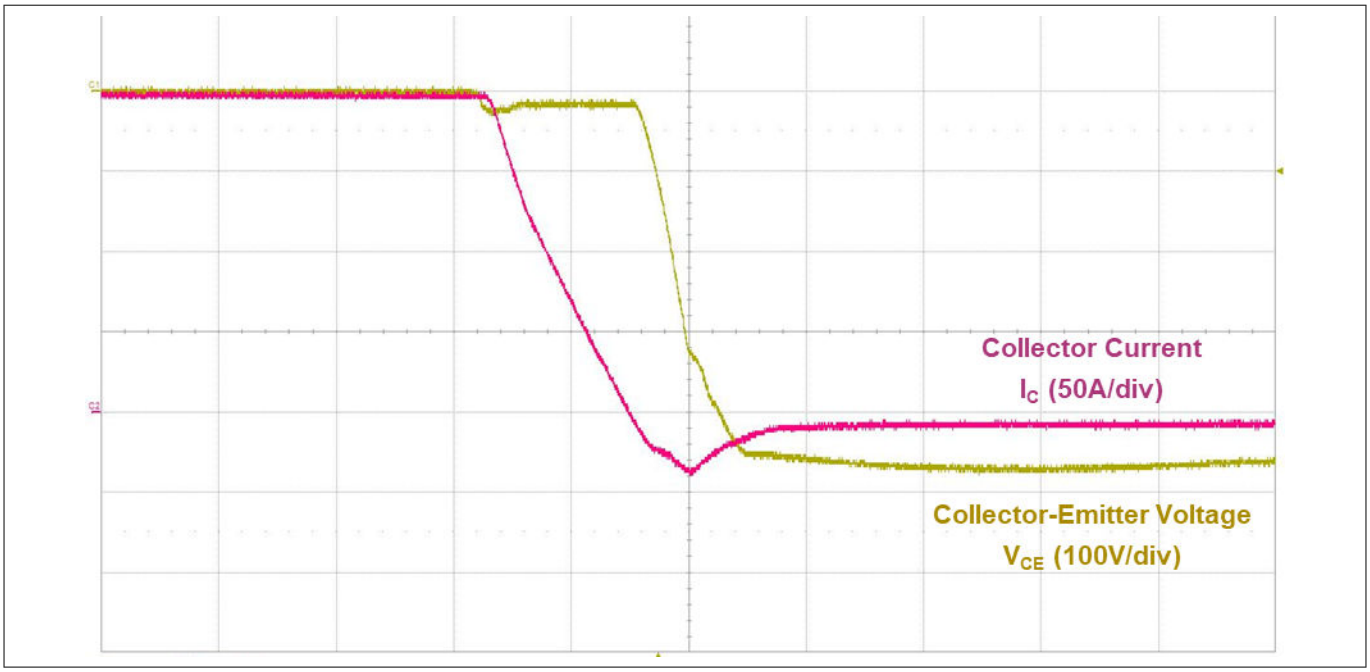

Figure 11 25°C switching waveforms for AIKQ200N75CP2 diode at 200 A and 470 V

Figure 12(a) shows the turn-on transient and Figure 12(b) shows the turn-off transient of AIKQ120N75CP2 IGBT at 25°C for a 120 A load current at a bus voltage of 470 V. The gate is driven by supply voltage from -8 V to +15 V, with the gate resistance of R_G = 5 Ω. The turn-on loss is 8.95 mJ. The collector current rate-of-change d*i*/d*t* during turn-on transient is approximately 0.7 A/ns and the collector-emitter voltage rate-of-change d*v*/d*t* is approximately 5.7 V/ns. The turn-off loss is 4.37 mJ. During turn-off, the collector current rate-of-change d*i*/d*t* is approximately 2.5 A/ns and the collector-emitter voltage rate-of-change is approximately 8.3 V/ns. The turn-off voltage overshoot peaks at approximately 600 V.

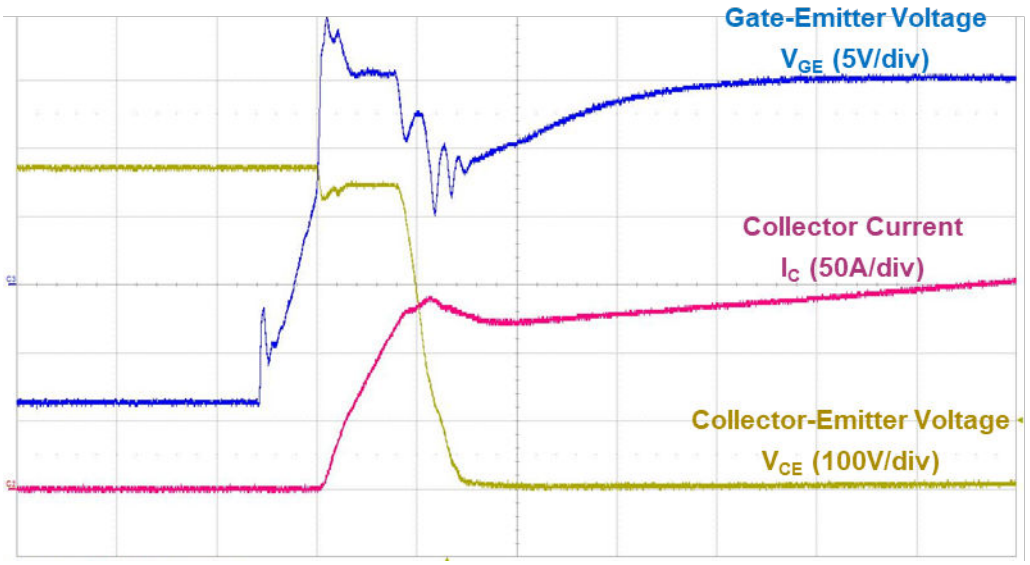

(a) Turn-on transient

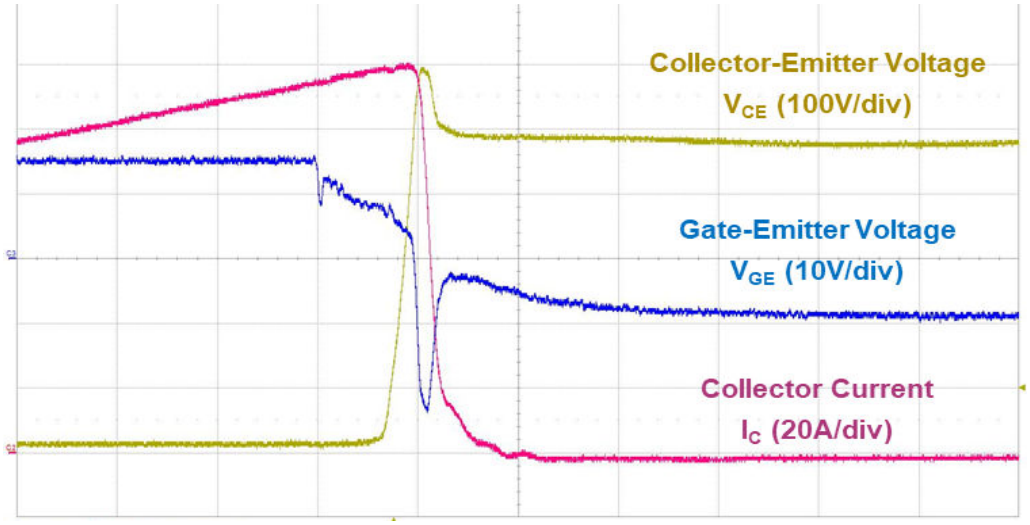

(b) Turn-off transient

Figure 12 25°C switching waveforms for AIKQ120N75CP2 IGBT at 200 A and 470 V

Figure 13 shows the high side diode's reverse recovery behavior during turn-on of the low side IGBT at 25°C. The peak reverse recovery current I_{rrm} is approximately 33 A. The reverse recovery charge is 3.5 µC and the energy loss is 1.07 mJ at 25°C.

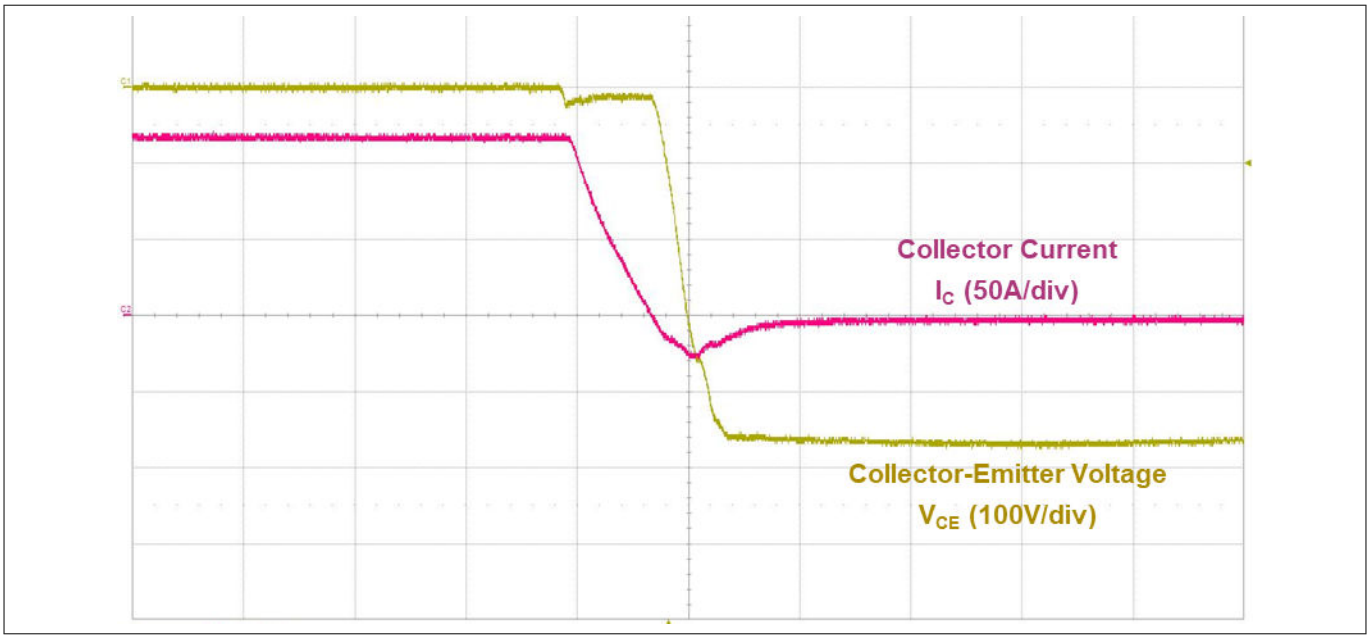

Figure 13 **25°C switching waveforms for AIKQ120N75CP2 diode at 200 A and 470 V**

3.3 Short-circuit behavior

The maximum short circuit withstand time of the AIKQ200N75CP2 t_{sc} is 5 µs at 25°C junction temperature with 470 V collector-emitter voltage. The gate driver voltage is from 0 V to 15 V with 4.8 Ω gate resistance. For safe operation, the allowed number of short-circuit events should be less than 1000 times and the time between each short-circuit event should be greater than 1 s.

High temperature short-circuit behavior is also estimated. Figure 14 illustrates the short-circuit measurement waveforms. Short-circuit current is 1075 A at 150°C junction temperature, all the other conditions are the same as described above. The average destruction energy is 2.25 J when the junction temperature is 150°C.

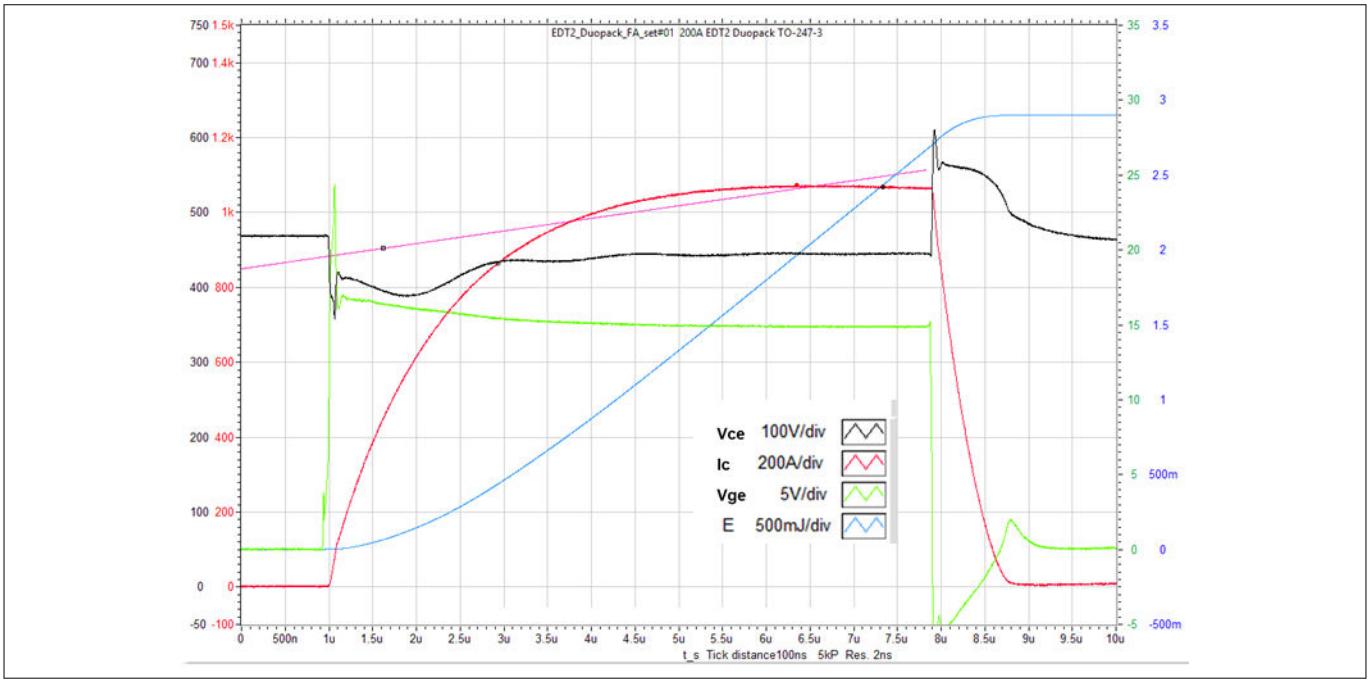

Figure 14 **Short-circuit test waveform of AIKQ200N75CP2**

3.4 Comparison of electrical behavior of AIKQ200N75CP2, AIKQ120N75CP2, and a 650 V 160 A at 25°C IGBT

AIKQ200N75CP2 provides outstanding high current capability as a discrete IGBT for the main inverter of electrical vehicles applications. The switching transient waveforms of AIKQ200N75CP2 and a 650 V 160 A at 25°C IGBT from a competitor are shown in Figure 15. The measurement is performed with the nominal current of each device, respectively.

The switching waveforms of the 650 V 160 A IGBT are measured with collector current at 160 A. The gate is driven by voltage from -8 V to +15 V with a 5 Ω gate resistor. Please note that the 650 V 160 A IGBT cannot be tested with the BUS voltage higher than 400 V, therefore the voltage applied onto the 650 V 160 A IGBT is limited at 400 V. The turn-on loss is 9.50 mJ compared to 20.42 mJ of the AIKQ200N75CP2 as explained above. However, please note that the switching losses of AIKQ200N75CP2 are measured under 470 V BUS voltage and 200 A collector current. The turn-off loss of the 650 V 160 A IGBT is 4.43 mJ compared to the 8.16 mJ of AIKQ200N75CP2 measured at 200 A collector current and 470 V collector-emitter voltage.

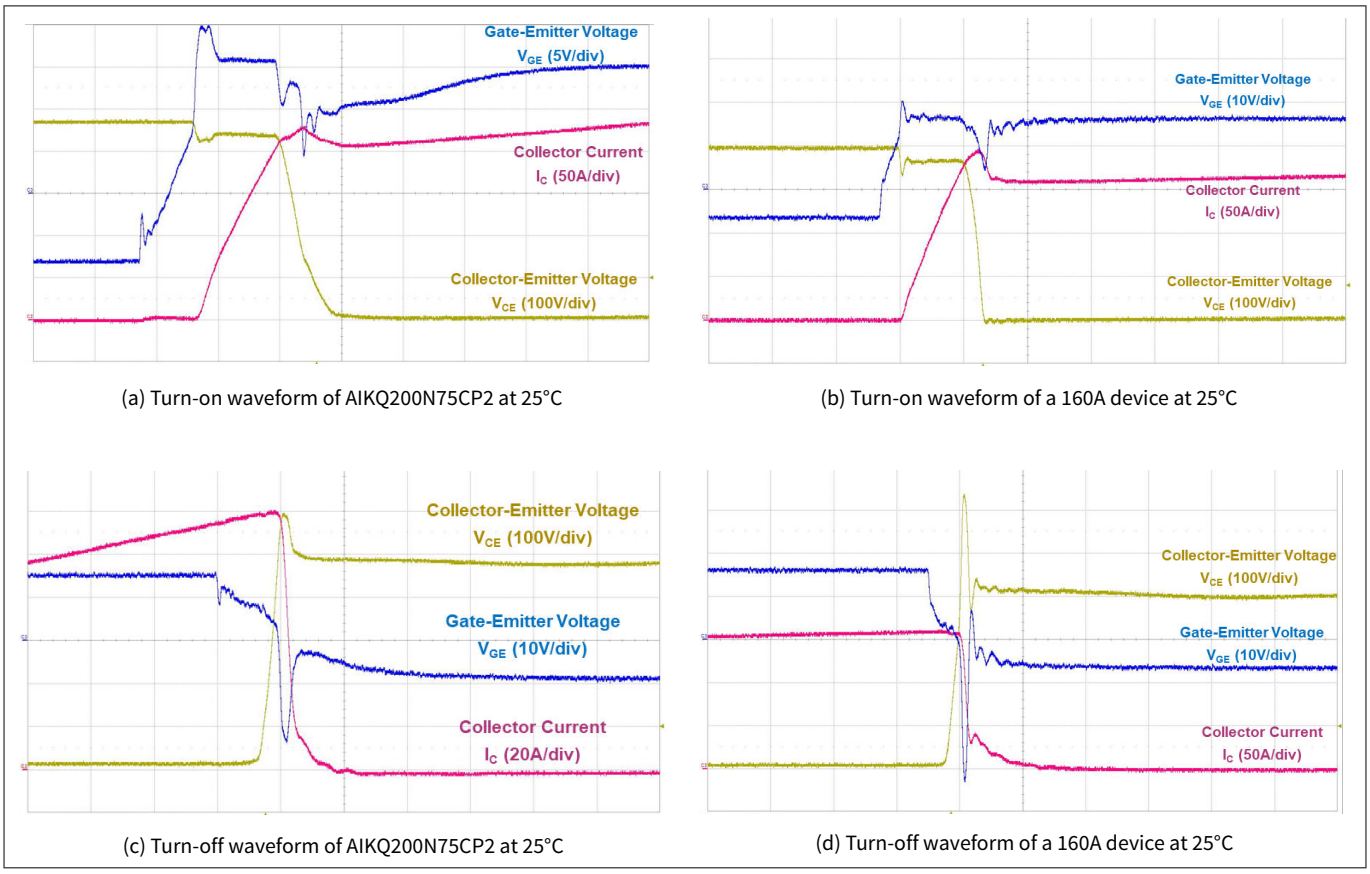

(a) Turn-on waveform of AIKQ200N75CP2 at 25°C

(b) Turn-on waveform of a 160A device at 25°C

(c) Turn-off waveform of AIKQ200N75CP2 at 25°C

(d) Turn-off waveform of a 160A device at 25°C

Figure 15 Comparison of switching behavior of AIKQ200N75CP2 and a 650 V 160 A IGBT

Wide open throttle (WOT) vehicle acceleration and deceleration – 95 mph simulations are performed on AIKQ200N75CP2, AIKQ120N75CP2, and the 650 V 160 A IGBT. The maximum operating current for each phase is 650 Arms. There are 5 AIKQ200N75CP2 devices in parallel for each switch so that the maximum operating current for each device is 130 Arms. For AIKQ120N75CP2 and the 650 V 160 A IGBT, there are 6 devices in parallel. Therefore, the maximum operating current for each device is 108 Arms. This is presented in Chapter 4.1.

3.5 Average power losses of a B6 inverter during one machine electrical cycle

A good methodology to compare the performance of different devices in an inverter application is the estimation of the average power losses in a system. For a sinusoidal PWM inverter, where the pulse pattern is generated by comparing a sinusoidal signal with a triangular carrier of frequency equal to f_{sw} and the first fundamental harmonic output or phase voltage is defined as V_{out} (referenced to the load virtual neutral point). Where I_{peak} is the peak output current $I_{peak} = \sqrt{2} \cdot I_{out}$ and the modulation factor is calculated as $m = V_{out}/(V_{DC}/2)$. If a value in the linear region $m \leq 1$ is considered and the power factor cos(ø) at the operation point is defined as positive for motoring conditions, and negative for regenerating conditions. The following methodology can be used to compare the performance of the system by assuming the following simplifications:

- All IGBTs and diodes behave like the typical values of the datasheet summing the same turn-on voltages, and commutation speeds fixed by the R_g and V_{ge} used in characterization
- The output frequency is significantly lower than the switching frequency $f_{sw} >> f_o$
- The output current ripple is not taken into consideration
- The average temperature T_j used for calculation is defined like in Figure 16

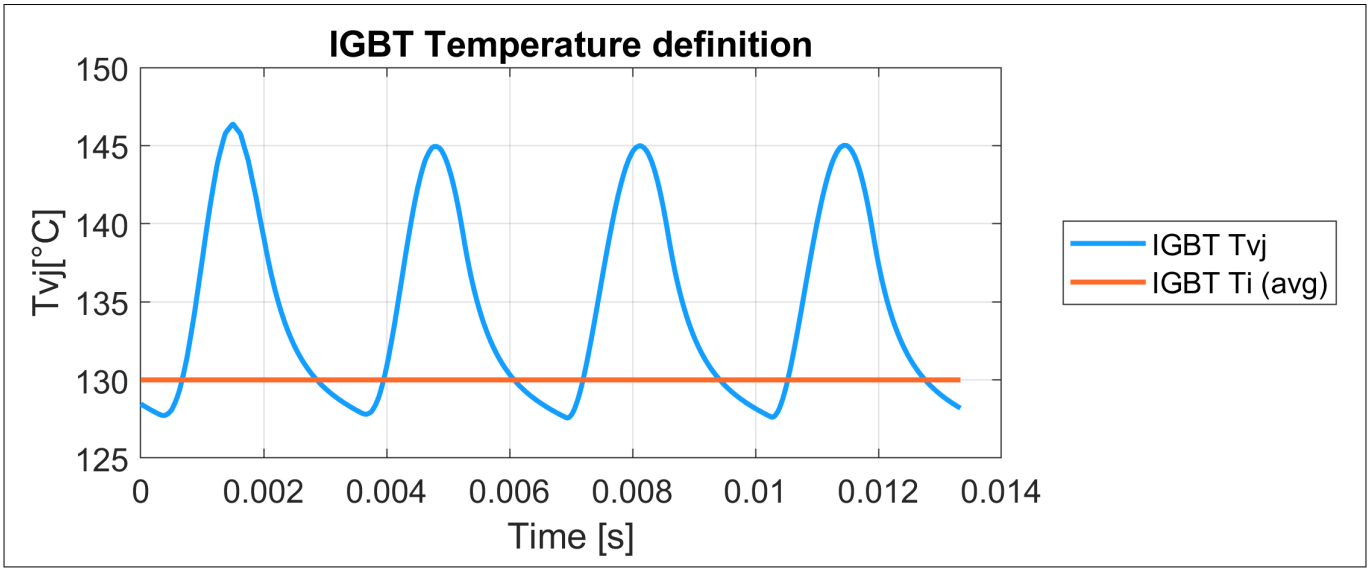

Figure 16 Example IGBT temperature and average temperature T_j (avg)

Under these assumptions, the only required information is all contained inside the Product Datasheet.

For the maximum motoring operating point and maximum regeneration condition, the following model can be used.

If a linear model is used to describe the device behavior devices:

$$V_{CESAT}(t) = V_{CE0} + R_{CE} I_C(t) = V_{CE0} + R_{CE} I_1 \sin(wt) \quad (1)$$

$$V_F(t) = V_{F0} + R_D I_F(t) = V_F + R_D I_1 \sin(wt) \quad (2)$$

Where saturation voltage V_{CE0} is the crossing of the linear model for the output characteristic with the x-axis and the forward voltage V_{F0} is the crossing of the linear model for the diode forward characteristic with the x-axis. The equivalent resistances if the IGBT R_{CE} and diode R_D are calculated as:

$$R_{CE} = \frac{(V_{CESAT}(2 \times I_c \text{ nom}) - V_{CESAT}(I_C \text{ nom}))}{I_c \text{ nom}} \tag{3}$$

$$R_D = \frac{(V_F(2 \times I_F \text{ nom}) - V_F(I_F \text{ nom}))}{I_c \text{ nom}} \tag{4}$$

The devices conduction losses for the IGBT and the diode in one electrical cycle can be estimated as:

$$P_{\text{cond IGBT}} = \left(\frac{1}{2\pi} + \frac{m \cos(\varphi)}{8}\right) V_{CE0}\left(T_j\right) I_{Peak} + \left(\frac{1}{8} + \frac{m \cos(\varphi)}{3\pi}\right) R_{CE}\left(T_j\right) I_{Peak}^2 \tag{5}$$

$$P_{\text{cond Diode}} = \left(\frac{1}{2\pi} - \frac{m \cos(\varphi)}{8}\right) V_{F0}\left(T_j\right) I_{Peak} + \left(\frac{1}{8} - \frac{m \cos(\varphi)}{3\pi}\right) R_D\left(T_j\right) I_{Peak}^2 \tag{6}$$

Similarly, the turn-on losses ($P_{\text{on IGBT}}$), turn off losses ($P_{\text{off IGBT}}$), and reverse recovery losses ($P_{\text{rr Diode}}$) can be estimated from the switching energies $E_{on}(I_{peak}, V_{DC}, T_{mean})$, $E_{off}(I_{peak}, V_{DC}, T_{mean})$, $E_{on}(I_{peak}, V_{DC}, T_{mean})$ as:

$$P_{\text{on IGBT}} = \frac{f_{sw}}{\pi} * E_{on}\left(I_{peak}, V_{DC}, T_{mean}\right) \tag{7}$$

$$P_{\text{off IGBT}} = \frac{f_{sw}}{\pi} * E_{off}\left(I_{peak}, V_{DC}, T_{mean}\right) \tag{8}$$

$$P_{\text{rr Diode}} = \frac{1}{\pi} \frac{f_{sw}}{} * E_{rr}\left(I_{peak}, V_{DC}, T_{mean}\right) \tag{9}$$

Where the temperature-dependent coefficients can be calculated based on the datasheet values at 25°C and 175°C as:

$$V_{CE0}\left(T_j\right) = \frac{V_{CE0}(25°C) - V_{CE0}(175°C)}{175 - 25}\left(T_j - 175\right) + V_{CE0}\left(175°C\right) \tag{10}$$

$$R_{CE}\left(T_j\right) = \frac{R_{CE}(25°C) - R_{CE}(175°C)}{175 - 25}\left(T_j - 175\right) + R_{CE}\left(175°C\right) \tag{11}$$

$$V_{F0}\left(T_j\right) = \frac{V_{F0}(25°C) - V_{F0}(175°C)}{175 - 25}\left(T_j - 175\right) + V_{F0}\left(175°C\right) \tag{12}$$

$$R_D\left(T_j\right) = \frac{R_D(25°C) - R_D(175°C)}{175 - 25}\left(T_j - 175\right) + R_D\left(175°C\right) \tag{13}$$

$$E_{on}\left(I_{peak}, V_{DC}, T_{mean}\right) = E_{on}\left(I_{nom}, V_{nom}, 175°C\right) \cdot \left(\frac{T_j + 273}{175 + 273}\right)^{\frac{\ln\left(\frac{E_{on}(I_{nom}, V_{nom}, 25°C)}{E_{on}(I_{nom}, V_{nom}, 175°C)}\right)}{\ln\left(\frac{298}{175+273}\right)}} \cdot \frac{I_{peak}}{I_{nom}} \cdot \frac{V}{V_{nom}} \tag{14}$$

$$E_{off}\left(I_{peak}, V_{DC}, T_{mean}\right) = E_{off}\left(I_{nom}, V_{nom}, 175°C\right) \cdot \left(\frac{T_j + 273}{175 + 273}\right)^{\frac{\ln\left(\frac{E_{off}(I_{nom}, V_{nom}, 25°C)}{E_{off}(I_{nom}, V_{nom}, 175°C)}\right)}{\ln\left(\frac{298}{175+273}\right)}} \cdot \frac{I_{peak}}{I_{nom}} \cdot \frac{V}{V_{nom}} \tag{15}$$

$$E_{rr}\left(I_{peak}, V_{DC}, T_{mean}\right) = E_{rr}\left(I_{nom}, V_{nom}, 175°C\right) \cdot \left(\frac{T_j + 273}{175 + 273}\right)^{\frac{\ln\left(\frac{E_{rr}(I_{nom}, V_{nom}, 25°C)}{E_{rr}(I_{nom}, V_{nom}, 175°C)}\right)}{\ln\left(\frac{298}{175+273}\right)}} \cdot \left(\frac{I_{peak}}{I_{nom}}\right)^{\frac{1}{2}} \cdot \frac{V}{V_{nom}} \tag{16}$$

To get a deeper inside into this model, the following literature is recommended [3].

3.5.1 Example 1. 160 KW inverter power losses and Rth requirement

For this example, a 160 KW inverter is considered. For a B6 Bridge topology with 650 A output RMS current and a 400 V DC link. Either 6 parallel switches of AIKQ120N75CP2, AIKQ120N60CT, a 160 A competitors' device, or 5 parallel switches of AIKQ200N75CP2 could be used. The target average operation temperature for the devices is selected as 130°C.

The operation conditions for each of the devices to be benchmarked are presented in Figure 17.

	Devices / SW	Io rms / Device	VDC	m	cos(ϕ)	f_{sw}	$T_{vj}\ avg$
Competitor 160A	6	108 [A]	400 [V]	0.9961	0.89	8 [kHz]	130 °C
AIKQ120N60CT	6	108 [A]	400 [V]	0.9961	0.89	8 [kHz]	130 °C
AIKQ120N75CP2	6	108 [A]	400 [V]	0.9961	0.89	8 [kHz]	130 °C
AIKQ200N75CP2	5	130 [A]	400 [V]	0.9961	0.89	8 [kHz]	130 °C

Figure 17 **Inverter device operation conditions. The output power of this inverter is 158 KW at this operations point. Please note that the competitor device used is a 650 V IGBT rated 160 A at 25°C but its I_c *nom* at 100°C is 120 A comparable to the AIKQ120N75CP2 and the AIKQ120N60CT**

To compare the different possible configurations, the power losses are to be determined. The power losses breakdown is calculated using equations (5) to (16). The results are presented in Figure 18 for the motoring condition and in Figure 20 for regenerating condition.

As shown in Figure 18 on the right side, when 130 Arms current is carried by AIKQ200N75CP2, the total average power loss is 131 W. The conducting losses of the IGBT are 69 W, turn-on loss is 28 W, and turn-off losses are 16 W. The diode conduction losses are 14 W and the reverse recovery losses are 4 W.

When AIKQ120N75CP2 is operating at 108 Arms collector current, the total average power losses sum 105 W. The conducting loss of the IGBT is 59 W, turn-on loss is 16 W, and turn-off loss is 12 W. The diode conduction losses are 13 W and the reverse recovery losses are 4 W.

In comparison, when the competitor 160 A IGBT is operating at 108 Arms, the average total power loss is 143 W, which is 39 W higher than AIKQ120N75CP2 when operating at the same conditions. The lower V_{ce} sat of the EDT2 devices reduces the conduction losses. And the Emitter-controlled diode with a small tail current reduces the turn-on losses as well as the reverse recovery losses. Ending up with 27% less power loss for this operation point.

When comparing the device with the previous generation the AIKQ120N60CT, again a 12% losses reduction is calculated. A lower conduction loss shows that the collector-emitter saturation voltage of AIKQ200N75CP2 and AIKQ120N75CP2 are significantly lower in the new generation.

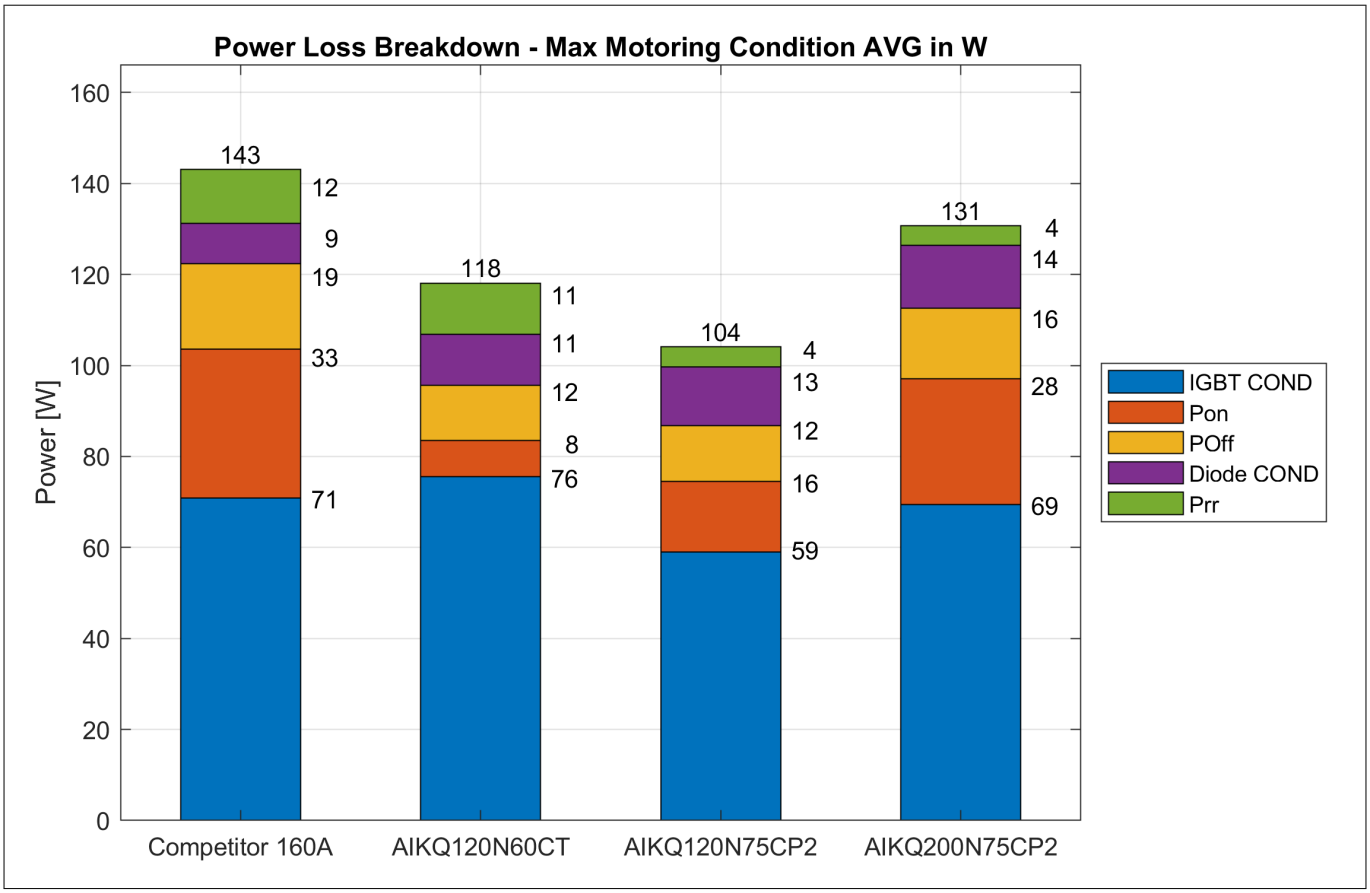

Figure 18 **Switching loss comparison per switch in motoring condition at AVG op temp = 130°C. Dc link voltage is 400 V and the total inverter output current is 650 A RMS. 6 pieces in parallel are used for the Competitor 160 A, the AIKQ120N60CT, and AIKQ120N75CP2 since they all have an I_c = 120 A at T_C = 100°C. 5 Pieces in parallel are considered for the AIKQ200N75CP2. The losses breakdown per device is shown**

Now, if the total losses are divided by the RMS current at the operation point, it is possible to benchmark all devices. These values are presented in Figure 19, now it is possible to see that the configuration with 5 AIKQ200N75CP2 devices also reduces the total losses by around 23%.

The losses per ampere in the EDT2 devices are close to 1 W/A RMS. In the previous generation, the AIKQ120N60CT losses sum 1.13 W/A RMS and the competitor device is around 1.41 W/A RMS.

This efficiency increase in motoring operation is part of the offering of EDT2 technology and has been one of the reasons why this technology has been so successful.

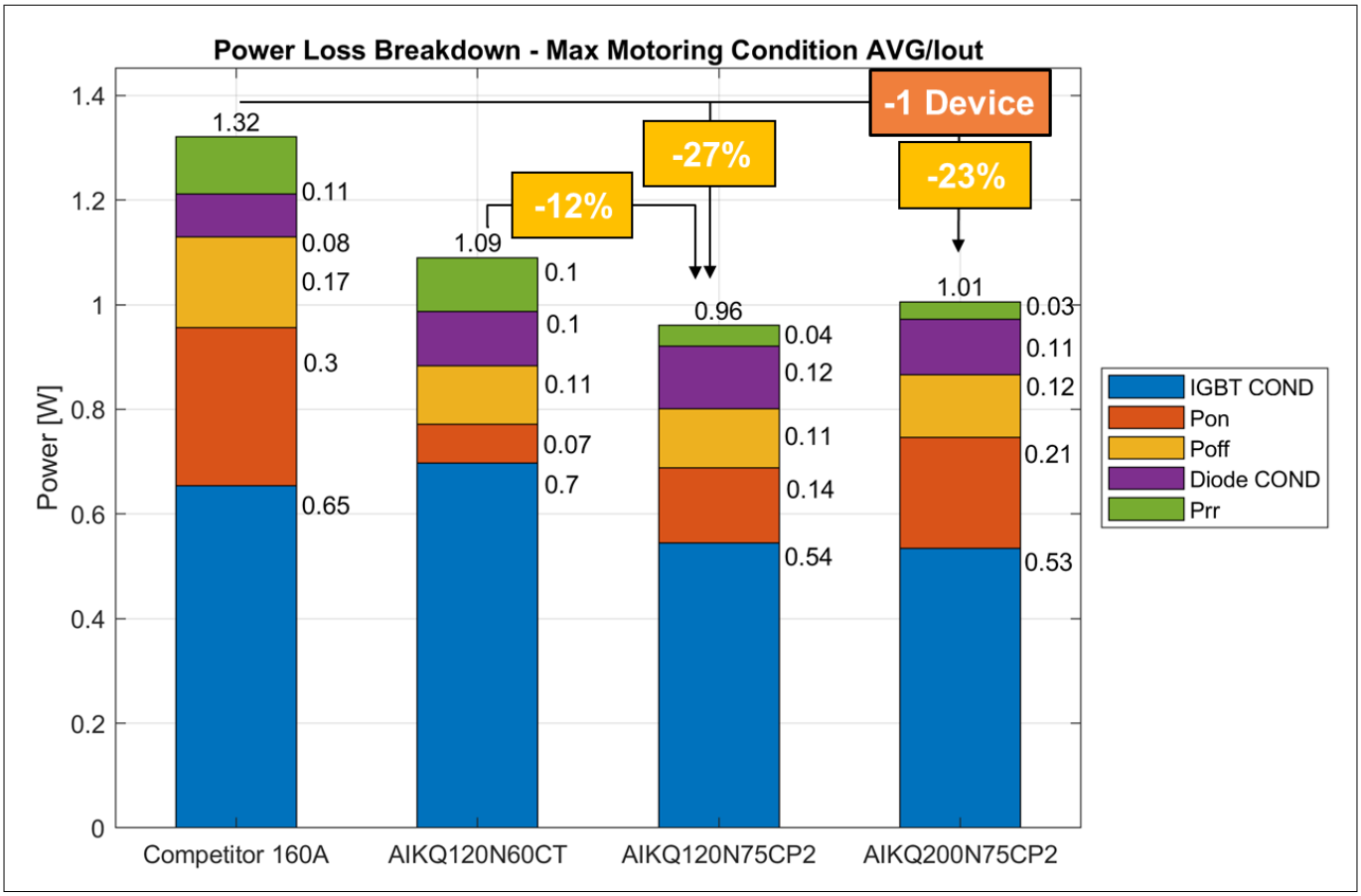

Figure 19 **Switching loss comparison per ampere for each switch in motoring condition at AVG op temp = 130°C. The DC link voltage is 400 V and the total inverter output current is 650 A RMS. The losses breakdown per RMS output ampere for each device is shown**

In Figure 20 the results for the regeneration condition are displayed. On the right side, when 130 Arms current is carried by AIKQ200N75CP2, the total average power loss is 143 W. The conducting losses of the IGBT are 11 W, turn-on loss is 28 W, and turn-off losses are 16 W. The diode conduction losses are 84 W and the reverse recovery losses are 4 W.

When 108 Arms current AIKQ120N75CP2 is operating at 108 Arms forward current, the total average power losses sum 122 W. The conducting loss of the IGBT is 10 W, turn-on loss is 16 W, and turn-off loss is 12 W. The diode conduction losses are 80 W and the reverse recovery losses are 4 W.

In comparison, when the competitor 650 V 160 A IGBT is operating at 108 Arms, the average total power loss is 127 W, which is 5 W higher than AIKQ120N75CP2 when operating at the same current. The Emitter-controlled diode with a small tail current reduces the turn-on losses as well as the reverse recovery losses. Ending up with 5% less power loss for this operation point.

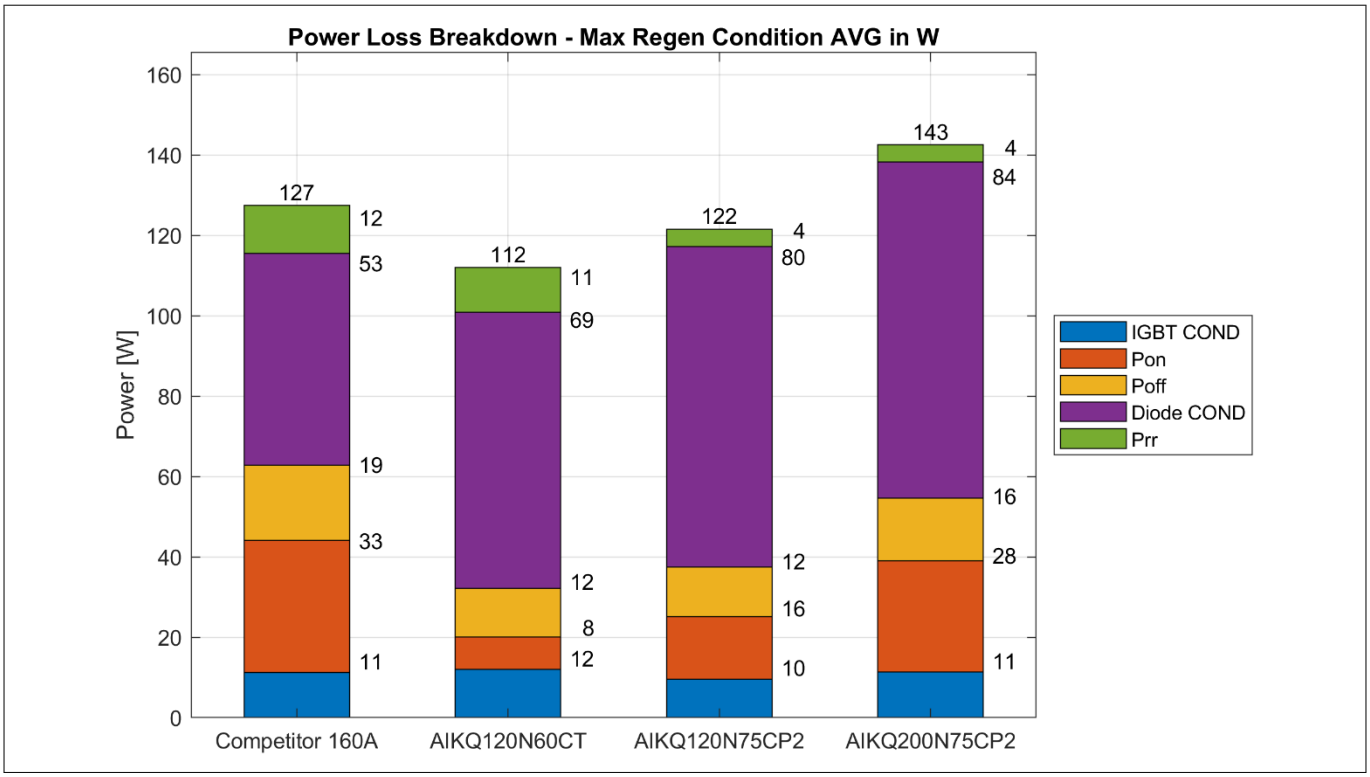

Figure 20 **Switching loss breakdown comparison for each switch in regenerating condition at AVG op temp = 135°C. The DC link voltage is 400 V and the total inverter output current is 650 A RMS. 5 Pieces in parallel are considered for the AIKQ200N75CP2 instead of 6 for the other cases**

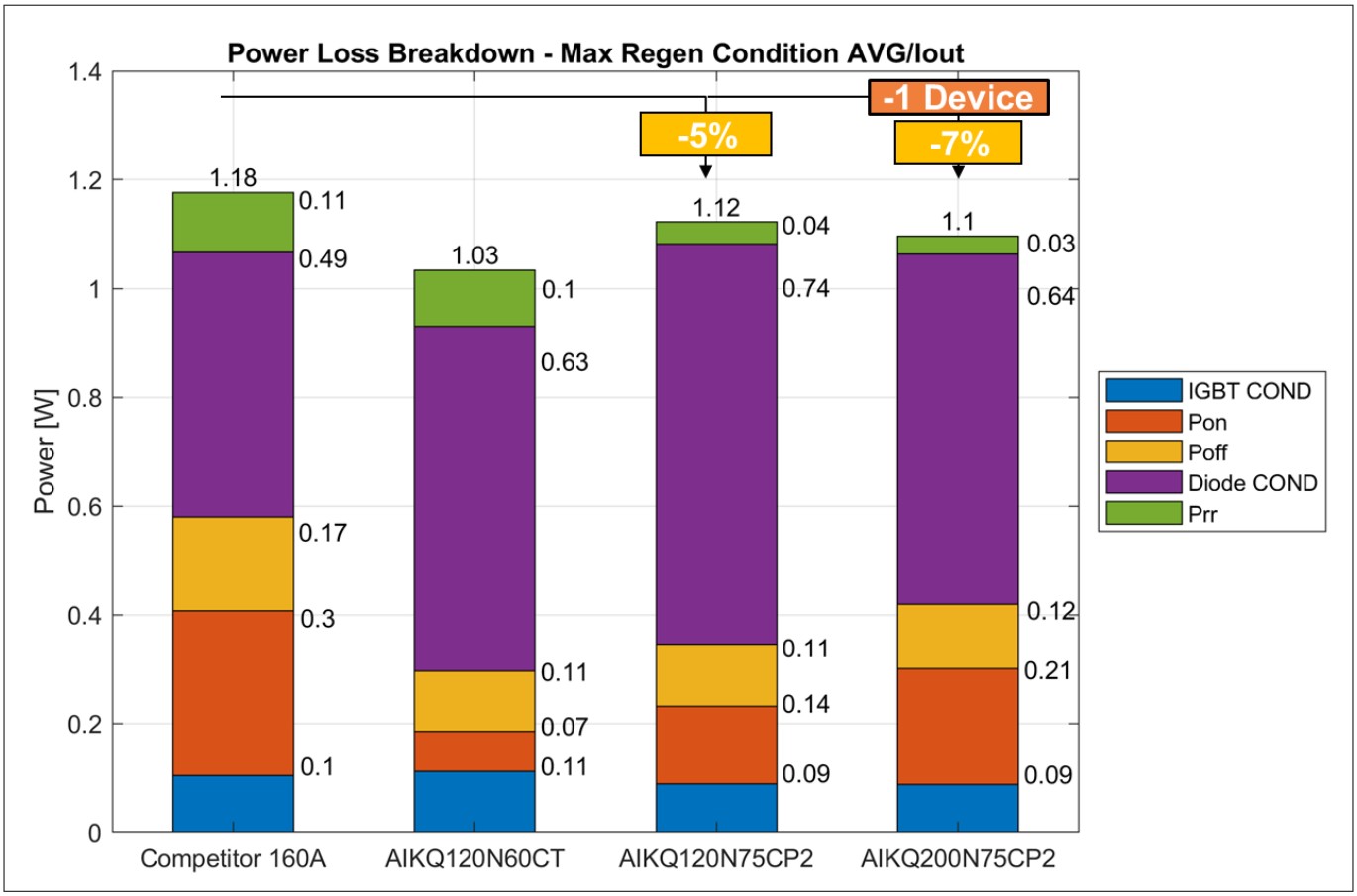

Figure 21 **Switching loss comparison per ampere for each switch in regenerating condition at AVG op temp = 130°C. The DC link voltage is 400 V and the total inverter output current is 650 A RMS. The losses breakdown per ampere for each device are shown**

Figure 21 shows the total device losses per ampere during regeneration. The losses per ampere in the EDT2 devices are close to 1.1 W/A RMS in regeneration conditions. The AIKQ200N75CP2 has 7% fewer losses than the Competitor device that has an average of 1.18 W/A RMS. In the previous generation, the AIKQ120N60CT is slightly more efficient in regeneration conditions with 0.09 W/A RMS fewer losses. This compromise is to reduce the tail current and enhance the motoring operation losses.

If we consider a 158 KW output power for the inverter. The efficiency of the system can be calculated as the output power divided by the input power. If we assume that the input power is the sum of the device's total losses and the output power, the system efficiency can be approximated.

These results are presented in Figure 22 and show that the highest efficiency 97.7% in motoring conditions is achieved with 6 parallel devices of AIKQ120N75CP2. Similarly, for the AIKQ200N75CP2 system, the efficiency is 97.6%. Around a 1% increase in efficiency is expected with both EDT2 devices in motoring condition.

In regeneration conditions, the 5 AIKQ200N75CP2 devices in parallel, have a 97.4% system efficiency and the AIKQ120N75CP2 has a 97.3%. In general, an improvement of around 0.1 % to 0.2% is compared to the competitor's device.

		Motoring		Regen	
System output power 160 kW	Devices / SW	System Losses	System Efficiency	System Losses	System Efficiency
Competitor 160A	6	5.1 [kW]	96.9%	4.6 [kW]	97.2%
AIKQ120N60CT	6	4.2 [kW]	97.3%	4.1 [kW]	97.5%
AIKQ120N75CP2	6	3.7 [kW]	97.7%	4.3 [kW]	97.3%
AIKQ200N75CP2	5	3.9 [kW]	97.6%	4.4 [kW]	97.4%

Figure 22 **158KW Inverter efficiencies with different devices for Motoring (red) and Regenerating (green) conditions. V_{dc} = 400 V, I_o *RMS* = 650 A, *ma* = 0.9961, *cos phi* = 0.89, T_{vj} *avg* = 130°C**

Based on the original assumption about the average operation temperature should not exceed T_{vj} *avg* = 130°C, the system requirement can be calculated from the power converter losses as:

$$R_{th\,System} = \Sigma R_{th_i} = \frac{T_{VJ}(Avg) - T_a}{P_v} \tag{17}$$

Where $R_{th\ System}$ is the system thermal resistance in K/W (sum of the R_{th_i} of the device and the cooling system) andP_v is the total average losses of the device (IGBT or Diode independently). And T_a is the coolant temperature. For this example, a T_a = 65°C is assumed. With equation (17) the total system R_{th} requirement is calculated and from it, the heatsink R_{th} can be calculated by subtracting the device R_{th}. The results of these calculations are displayed in Figure 23.

			Motoring				Regen			
160 kW	N dev	Tvj avg [°C]	Syst. Loss. [kW]	Rth [K/W]	Dev. Rth [K/W]	HS. Rth [K/W]	Syst. Loss. [kW]	Syst. Rth [K/W]	Dev. Rth [K/W]	HS. Rth [K/W]
Competitor 160A	6	130	5.10	0.49	0.17	0.32	4.60	0.93	0.32	0.61
AIKQ120N60CT	6	130	4.20	0.63	0.2	0.43	4.10	0.75	0.45	0.30
AIKQ120N75CP2	6	130	3.70	0.69	0.22	0.47	4.30	0.71	0.40	0.31
AIKQ200N75CP2	5	130	3.90	0.53	0.14	0.39	4.40	0.68	0.26	0.42

Figure 23 **158 KW Inverter thermal system requirements with different devices for Motoring (red) and Regenerating (green) conditions. V_{dc} = 400 V, I_o *RMS* = 650 A, *ma* = 0.9961, *cos phi* = 0.89, T_{vj} *avg* = 130°C**

The R_{th} required for the heatsinks of the AIKQ120N75CP2 and the AIKQ200N75CP2 is 0.69 [K/W] and 0.53 [K/W] respectively. In comparison, the R_{th} required to maintain the same operating temperature in the 160 A Competitor device is 0.49 [K/W]. A to reach a lower system T_{th} the complexity of the cooling system must increase; more expensive materials and assembly mechanisms need to be used.

When comparing the previous generation AIKQ120N60CT with the AIKQ120N75CP2, also relaxed by a factor of around 0.06 [K/W] confirming the drop-in replacement capability of the new generation.

For the regeneration condition, EDT2 devices show also a more relaxed R_{th} requirement, compared to the previous generation this is due to the higher efficiency. A higher R_{th} requirement implies a lower thermal conductivity requirement for the heatsink.

Note: *The competitor R_{th} requirement is quite unbalanced, requiring much better cooling for the IGBT compared to the diode. Since both IGBT and Diode thermal systems are in a single device the smallest R_{th} will become the system requirement. Therefore, the Heatsink R_{th} for the competitor device system will be around 0.32 [K/W].*

The overall drop-in replacement capability is also notable here since all of the EDT2 devices can use the cooling systems of either the 160 A competitor or the previous generation devices. The R_{th} requirement is for all cases higher or equal in the EDT2 family compared to the other devices.

3.5.2 Example 2. Increase of power with the new EDT2 device generation

For this example, the operation conditions for the inverter are v_{dc} = 400V, *ma* = 0.9961, *cos phi* = 0.89. and the usage of either 6 parallel switches of AIKQ120N75CP2, AIKQ160N75CP2 or 160 A competitors' devices will be benchmarked. An operation temperature of T_v *avg* = 130°C and a coolant temperature of T_a = 65°C are defined. The target is to determine the maximum possible I_o RMS the system could deliver with each of the configurations.

The heatsink R_{th} is assumed to be 0.45 [k/W] and equal for all devices to benchmark. The resulting different R_{th} configurations for each of the devices to be benchmarked are shown in Figure 24.

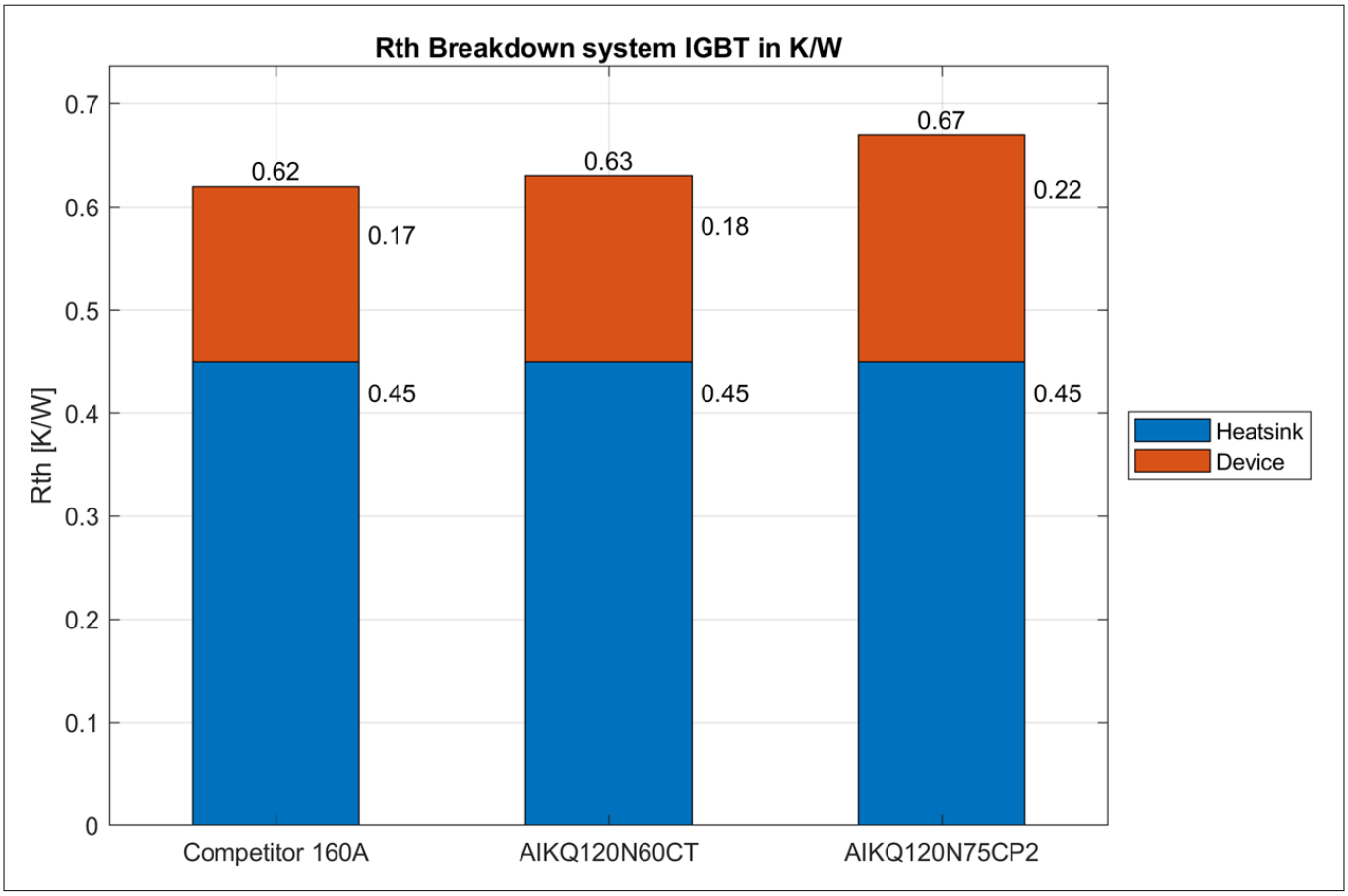

Figure 24 **Cooling system Rth for different devices, (Blue) Heatsink, (Orange)device, on top the sum of both systems**

For a certain system R_{th} and according to equation (17) the maximum power losses the thermal system can allow for a certain operation temperature and coolant temperature can be defined as:

$$p_v\max = \frac{T_{vj}(Avg) - T_a}{\Sigma R_{th_i}} \tag{18}$$

The maximum output power possible is the equilibrium between the thermal system described in (17) and the total losses in the die. And can be e expressed as:

$$p_v\max = p_{cond\,IGBT} + p_{offIGBT} + p_{on\,IGBT} \tag{19}$$

If we replace in (19) equations (5),(7),(8),(15) and (16) we can solve for the current arriving to the values presented in Figure 25. This value is the maximum possible RMS output current we can drive with the defined thermal system.

As shown in Figure 25 if the AIKQ120N75CP2 is taken as a drop-in replacement in the same cooling system, the maximum possible RMS output current increases by 21% compared to the competitor 160 A device, and 3.5% compared to the previous generation.

The losses breakdown at this operation point is shown in Figure 26, a 21% and an 11% loss reduction per ampere is obtained and therefore a total system efficiency increase is expected. The results of the system benefits are presented in Figure 27 and Figure 28.

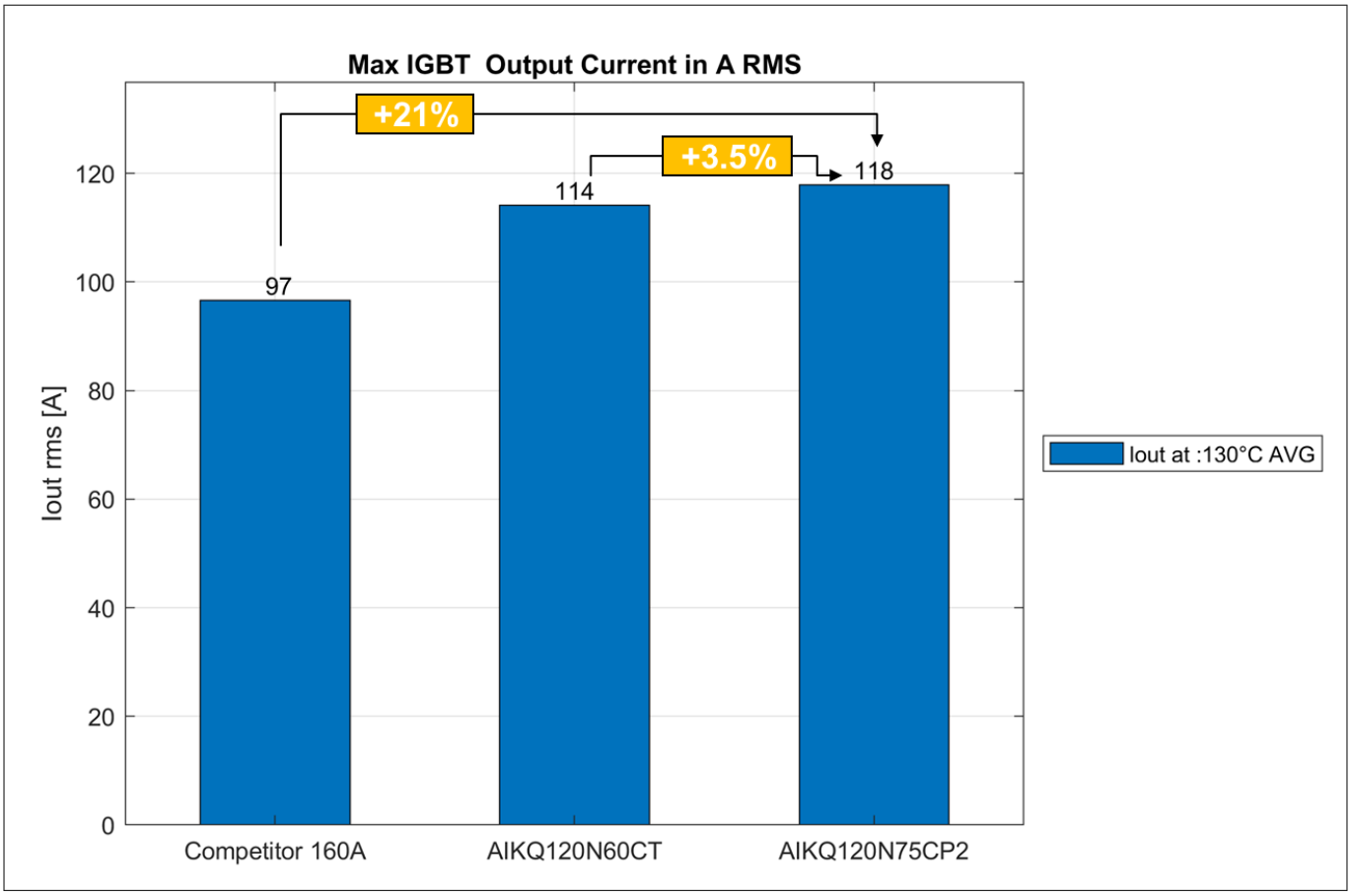

Figure 25 **Device Maximum output current (Blue) and Efficiency (orange) with each device configuration. V_{dc} = 400 V, *ma* = 0.9961, *cos phi* = 0.89, T_{vj} *avg* = 130°C**

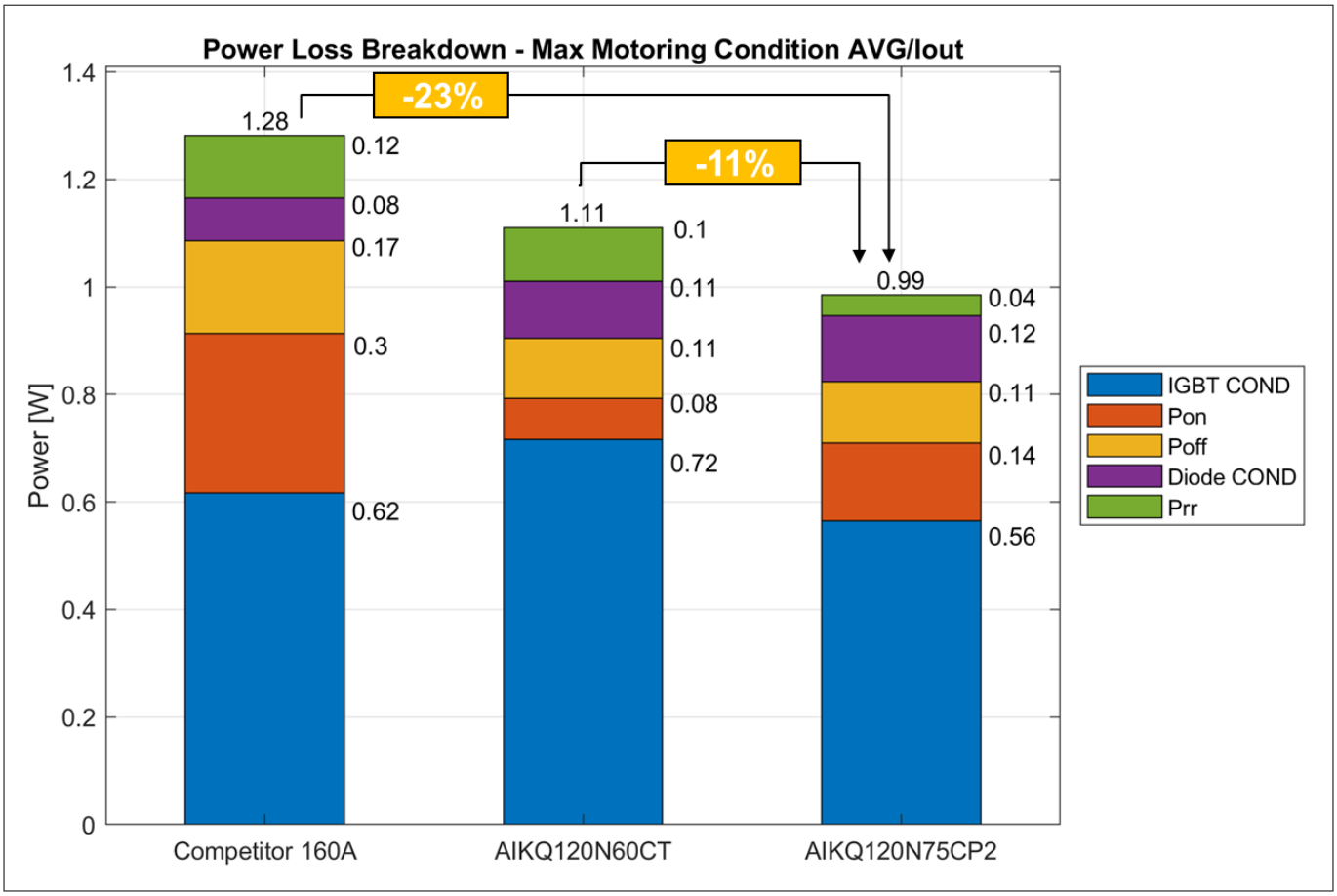

Figure 26 **Losses breakdown with each device per ampere at the maximum power operation point. V_{dc} = 400 V, *ma* = 0.9961, *cos phi* = 0.89, T_{vj} *avg* = 130°C**

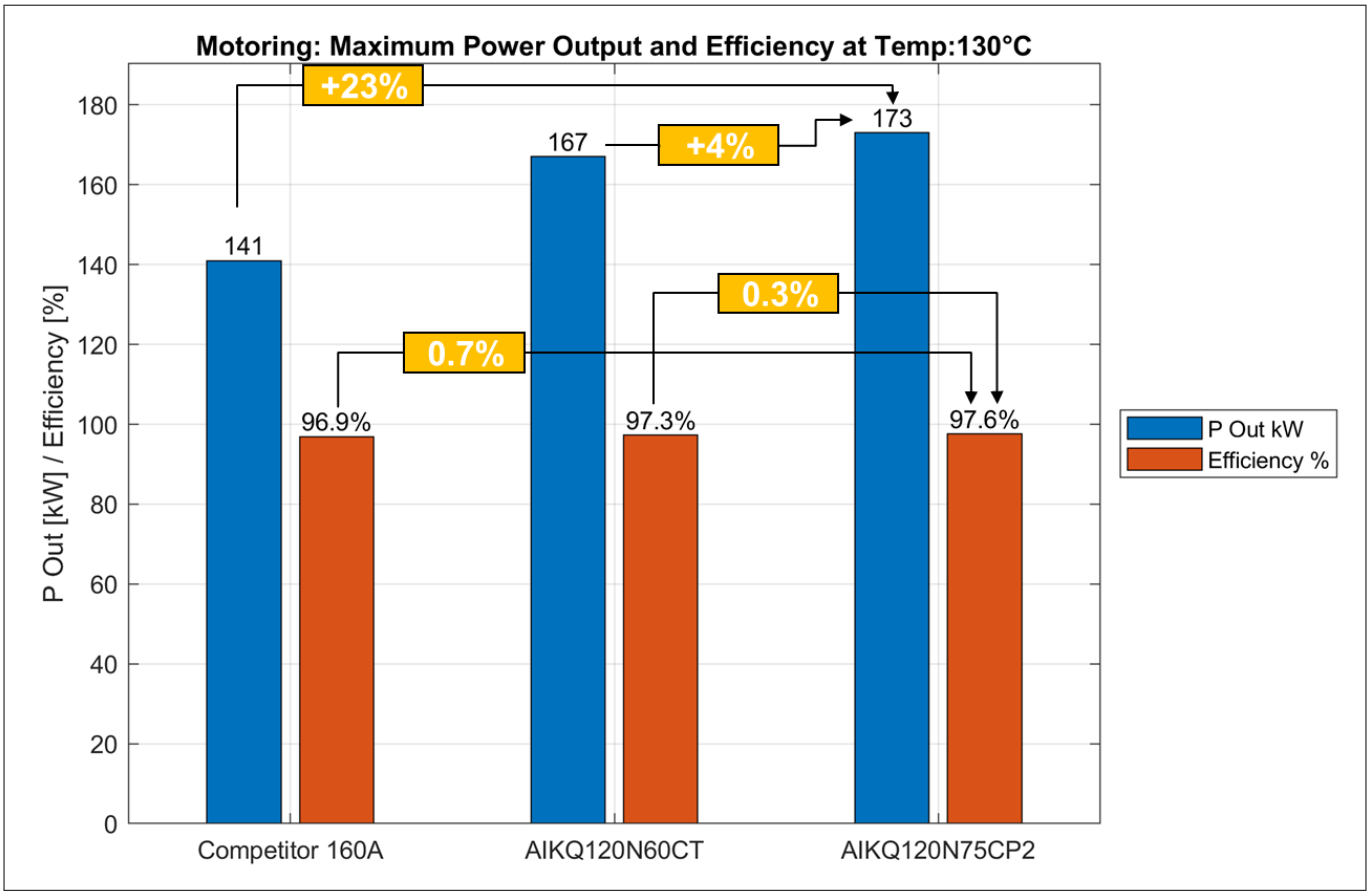

Figure 27 **Inverter maximum output power (blue) and efficiency (orange) with each device configuration. V_{dc} = 400 V, *ma* = 0.9961, *cos phi* = 0.89, T_{vj} *avg* = 130°C**

	Device			System			
	Nr Parallel dev	Tvj AVG [°C]	Iout Rms [A]	Total Losses [kW]	max Output Power [kW]	Efficiency [%]	Iout max RMS [A]
Competitor 160A	6	130	97	4.5	141	96.9	580
AIKQ120N60CT	6	130	114	4.6	167	97.3	684
AIKQ120N75CP2	6	130	118	4.3	173	97.6	707

Figure 28 **Inverter system specs with different devices for motoring condition. Values per device in (red) and for the system in (green). Operation conditions: V_{dc} = 400 V, Heatsink R_{th} = 0.45 [K/W], *ma* = 0.9961, *cos phi* = 0.89, T_{vj} *avg* = 130°C**

Figure 27 shows a power output increase of 23% and 4% when replacing the competitor device and the previous generation respectively. Also, an efficiency improvement of 0.7% and 0.3% are obtained respectively.

This shows the value of implementing the EDT2 chipset in the system. Finally, in Figure 28 we can see all values summarized.

3.5.3 Example 3. Comparison between 400 V vs 470 V systems

As explained in the previous section the maximum output power can be easily calculated for a defined configuration. In this section, the power output and efficiency increase obtained at 400 V and 470 V for the EDT2 devices is benchmarked. The device operation conditions are V_{dc} = 400 V and 470 V, *ma* = 0.9961, *cos phi* = 0.89. The system $R_{th}$are 0.68 [K/W] and 0,54 [K/W] for the 120 A and 200 A devices respectively. The operation conditions and results are summarized in Figure 29 and Figure 30.

	Device					System			
	VDC [V]	Nr Parallel dev	Tvj AVG [°C]	Iout RMS [A]	Rth j_w [K/W]	Total Losses [W]	max Output Power [kW]	Efficiency [%]	Iout max RMS [A]
AIKQ120N75CP2	400	4	130	116	0.68	2.7	114	97.6	466
AIKQ120N75CP2	470	4	130	112	0.68	2.7	129	97.9	447
AIKQ200N75CP2	400	4	140	152	0.54	3.8	149	97.5	608
AIKQ200N75CP2	470	4	140	145	0.54	3.8	166	97.7	579

Figure 29 **Inverter maximum output power (blue) and efficiency (orange) with each device configuration. V_{dc} = 400 V vs V_{dc} = 470 V, *ma* = 0.9961, *cos phi* = 0.89**

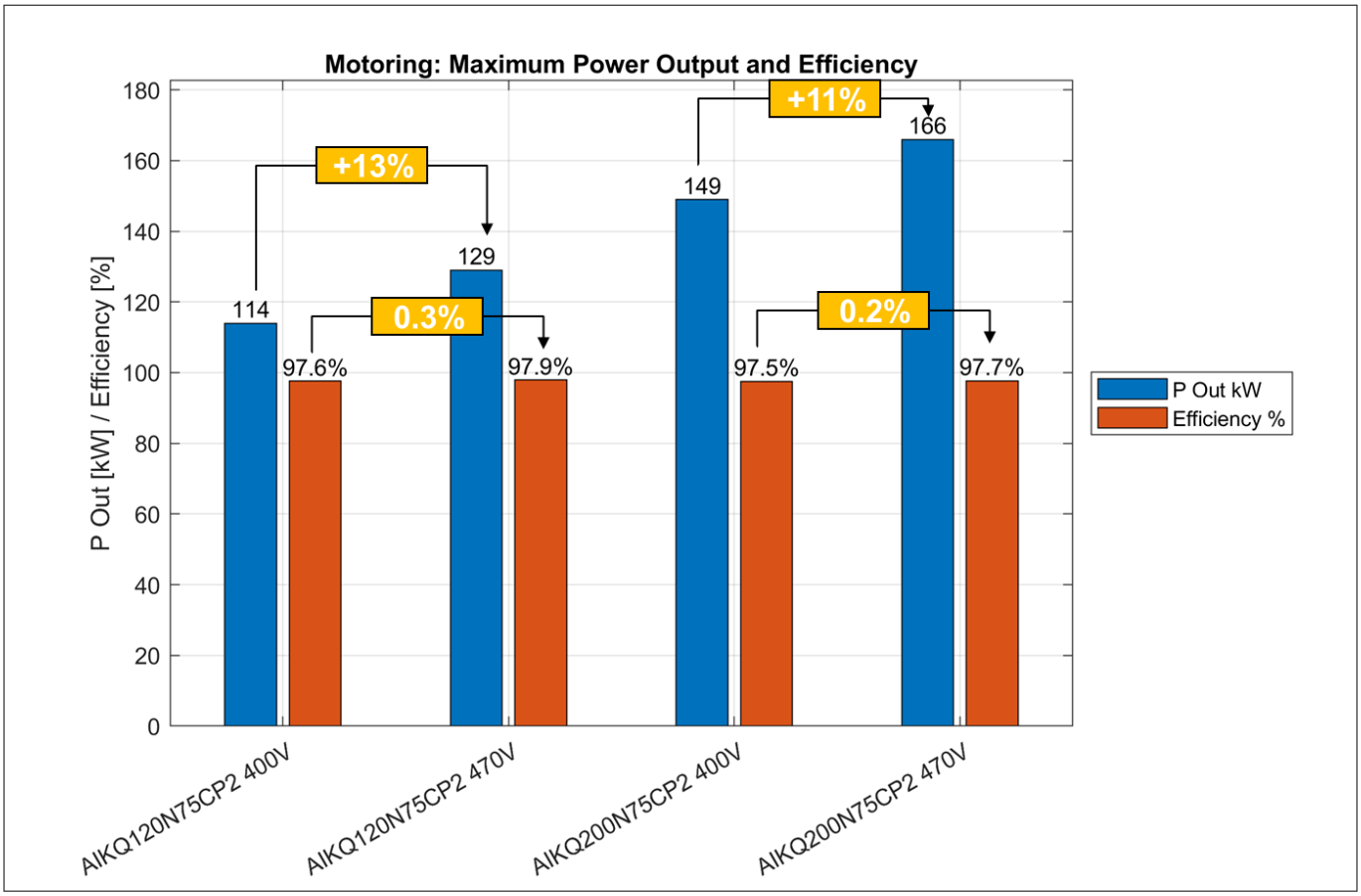

Figure 30 **158 KW Inverter thermal system requirements with different devices for Motoring (red) and Regenerating (green) conditions. V_{dc} = 400 V, I_o RMS = 650 A, *ma* = 0.9961, *cos phi* = 0.89**

Figure 29 and Figure 30 show that a total power output increase of 13% and 11% can be obtained by simply increasing the bus voltage to 470 V. The competitor device of the previous example as well as the previous generation can not operate at this range reliably. And this comparison with those systems does not make sense.

Another important point to highlight is that when increasing the bus voltage, the efficiency of the system increases around 0.3% to 0.4% when the voltage is raised. Similar to any high voltage system the losses decrease for the same output power at a higher voltage and there the system can put more power out without exceeding the thermal operating conditions.

3.6 Device paralleling of AIKQ200N75CP2

As discussed above, paralleling power devices increases the current capability of a system, which is important to the main inverters of electric vehicles. The paralleling simulation is performed to estimate the current sharing behavior of AIKQ200N75CP2 devices from the same lot. The simulation circuit is a half-bridge system with 4 pieces of AIKQ200N75CP2 – 2 devices on the high side to provide a freewheeling path and the other 2 devices on the low side as DUT.

The collector-emitter saturation voltage ($V_{CE\text{-}sat}$) distribution of the lot is approximately from 1.32 V to 1.36 V. The gate threshold voltage ($V_{GE\text{-}th}$) distribution of the same lot is approximately from 5.62 V to 5.86 V. Setup the IGBT models with the extreme parameters in the lot (IGBT-1 with $V_{CE\text{-}sat}$ = 1.32 V and $V_{GE\text{-}th}$ = 5.62; IGBT-2 with $V_{CE\text{-}sat}$ = 1.36 V and $V_{GE\text{-}th}$ = 5.86). A 500 µs 15 V pulse signal is applied synchronously to both of these two IGBTs. A 400 A DC source is connected to the half-bridge.

The results are shown in Figure 31. The current mismatch during conducting state is 1.79%. Turn-on energy loss mismatch is approximately 3% and turn-off energy loss is approximately 6%. The simulation results indicate that paralleling AIKQ200N75CP2 devices from the same lot behave safely under paralleling.

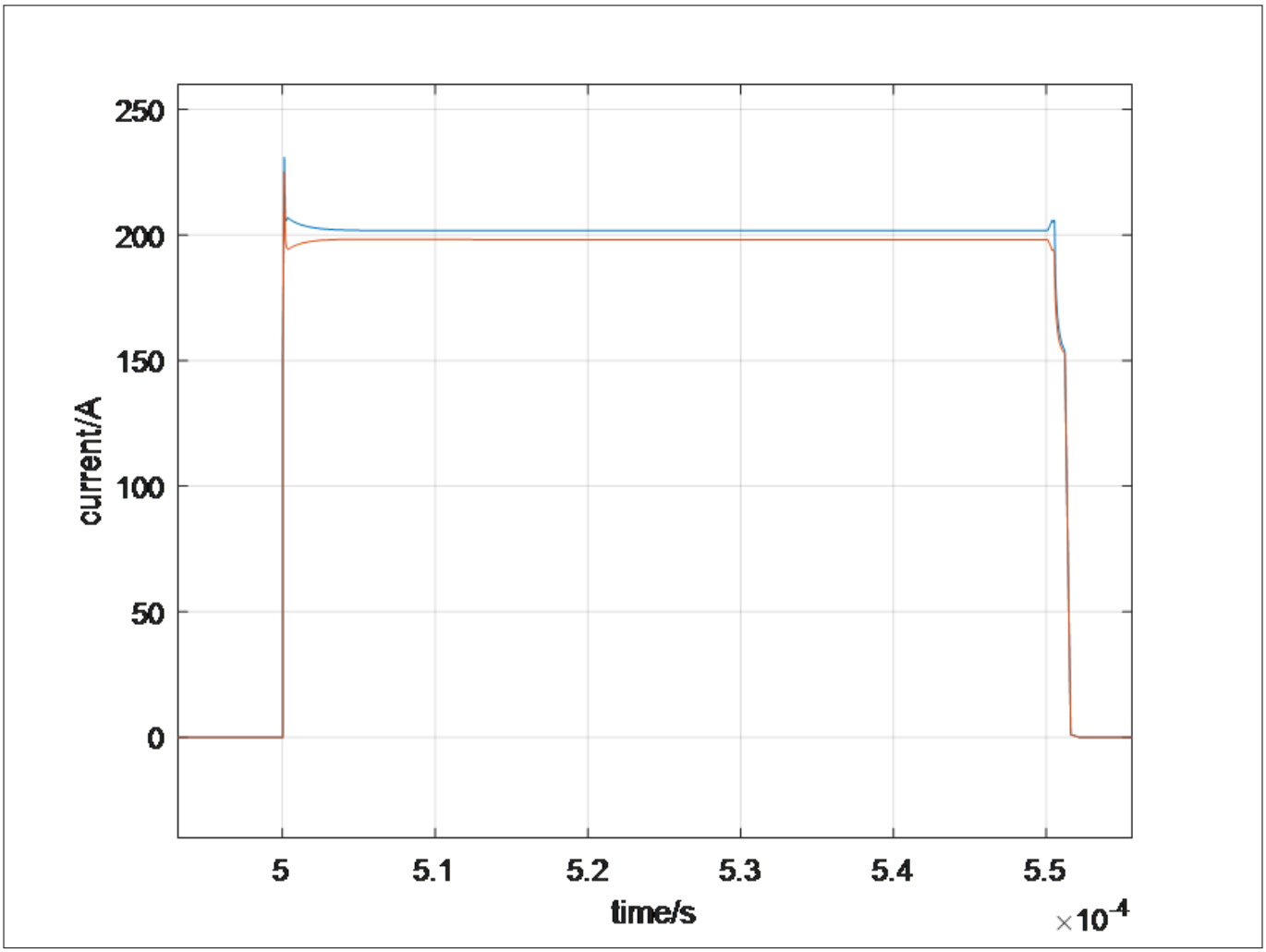

Figure 31 Current sharing behavior of paralleling AIKQ200N75CP2

Some designs with tighter parameter mismatch requirements, like systems with a high number of parallel devices per switch, can also be addressed with the AIKQ200N75CP2 or the AIKQ120N75CP2.

4 Typical high-power traction application

Wide Open Throttle (WOT) Vehicle Acceleration and Deceleration – 95 mph simulations are performed on AIKQ200N75CP2, AIKQ120N75CP2, and the 650 V 160 A IGBT. The maximum operating current for each phase is 650 Arms. There are 5 AIKQ200N75CP2 devices in parallel for each switch so that the maximum operating current for each device is 130 Arms. For AIKQ120N75CP2 and the 650 V 160 A IGBT, there are 6 devices in parallel. Therefore, the maximum operating current for each device is 108 Arms.

4.1 Application

Several groups of application simulations are performed to estimate the performance of AIKQ200N75CP2. The results of Wide-Open Throttle (WOT) Vehicle Acceleration and Deceleration – 95 mph simulations are shown in the below figure.Figure 32 (a) shows the phase-phase voltage and the single device current. Figure 32 (b) shows the junction temperature and instant power losses of IGBT and diode. The vehicle model and propulsion system restrict the maximum current of each device at 130 Arms. DC BUS voltage is 450 V. The switching frequency is 10 kHz. The coolant temperature is 65°C. With the assumption that the cooling system is with typical parameters, the maximum temperature of the IGBT chip is 148°C and of the diode is 144°C. There is enough margin of junction temperatures during WOT operating.

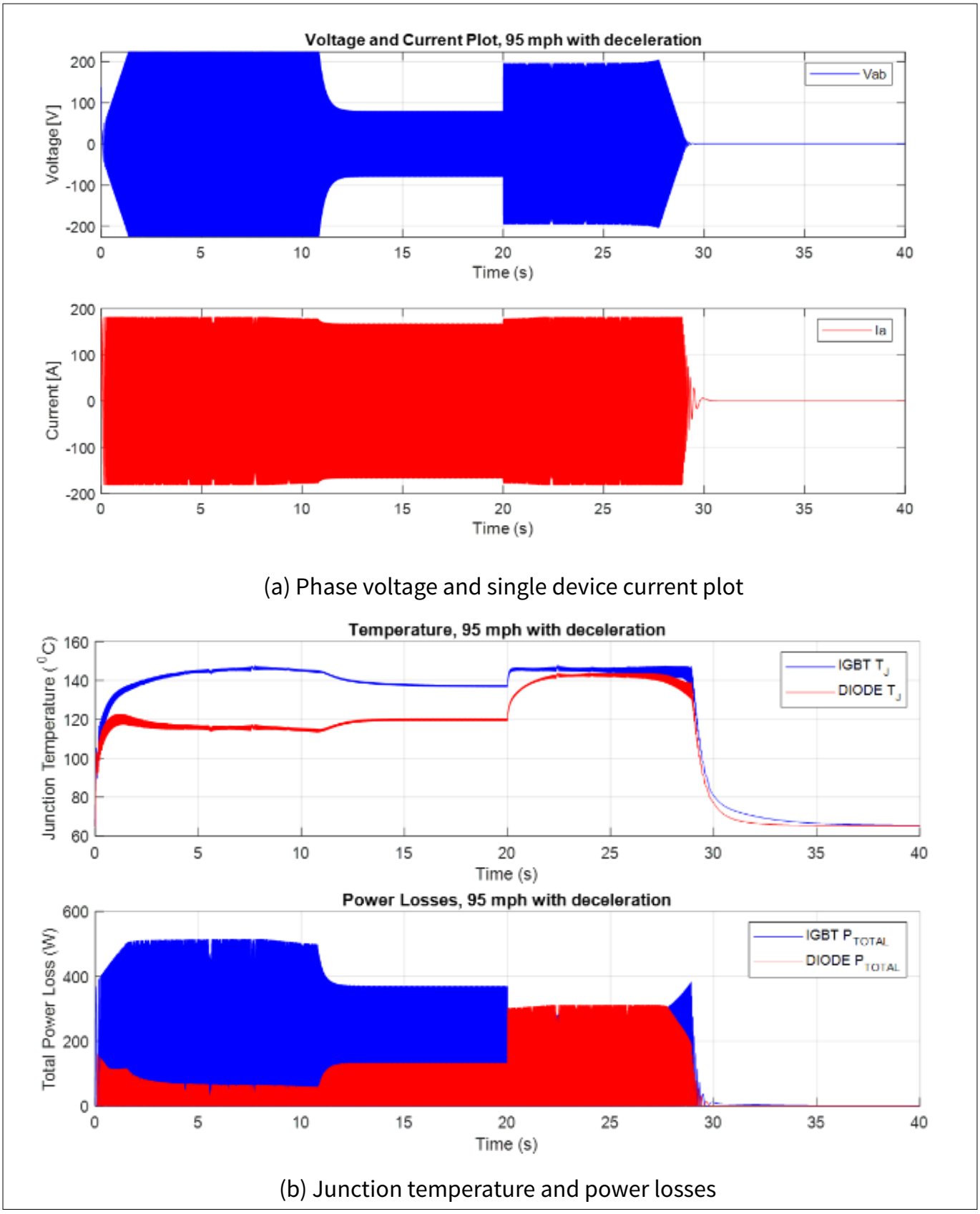

Figure 32 Simulation results of WOT – 95 mph

To estimate the life span consumption in real applications, simulations on the United States Environmental Protection Agency (EPA) Drive Cycle for Light Passenger Vehicle profile have been performed. The profile

consists of 3 types of drive cycle: Urban Dynamometer Driving Schedule (UDDS, Figure 33 (a)), US06 (Figure 33 (b)), and Highway Fuel Economy Driving Schedule (HWFET, Figure 33 (c)). As shown in Table 2, the drive length of UDDS, US06, and HWFET are 1369 seconds, 596 seconds, and 765 seconds, respectively. The drive distances of them are 7.45 miles, 8.01 miles, and 10.26 miles, respectively. The average speeds are 19.59 mph, 48.37 mph, and 48.30 mph.

Table 2 Characteristics of each EPA drive cycle

Individual EPA drive cycles used			
	Length (sec)	**Distance (mi)**	**Avg Speed (mph)**
UDDS	1369	7.45	19.59
US06	596	8.01	48.37
HWFET	765	10.26	48.30

The one-year use of the EPA drive cycle for light passenger vehicles is shown in Table 3. Trips are classed into three types: work, errand, and weekend/vacation. Each drive trip consists of several drive cycles. In Chapter 4.2, the thermal response of the device for each drive cycle is described. Based on the thermal response and Table 3, the thermal cycle and life span of one-year consumption of the device will be analyzed in Chapter 4.3.

Table 3 One-year usage of each light passenger vehicle

Individual trips				
Trip	**Frequency**	**Drive cycle combos**	**Sub trips**	**Represents**
Work	Twice daily, 5 days/wk. 48 wk./yr.	UDDS + US06	A	Commute to work after the full overnight charge (always); Also applicable for commute home after fully charged at work (5% likelihood)
			B	Commute home after no recharging while at work (95% likelihood)
Errand	3 days/wk. 48 wk./yr.	UDDS	A	Evening round trip after fully recharged at home (15% likelihood)
			B	Evening round trip starting at same SOC as when returned from Trip 1 (85% likelihood) (recharged at work)
			C	Evening round trip starting at same SOC as when returned from Trip 1 (85% likelihood) (did not charge at work)
Weekend or vacation	124 days/yr.	UDDS + HWFET + HWFET + HWFET + HWFET + UDDS	A	Weekend round trips after the full overnight charge (95% likelihood)
		UDDS + HWFET + HEFET	B	Weekend trip one way after a full recharge (5% likelihood)

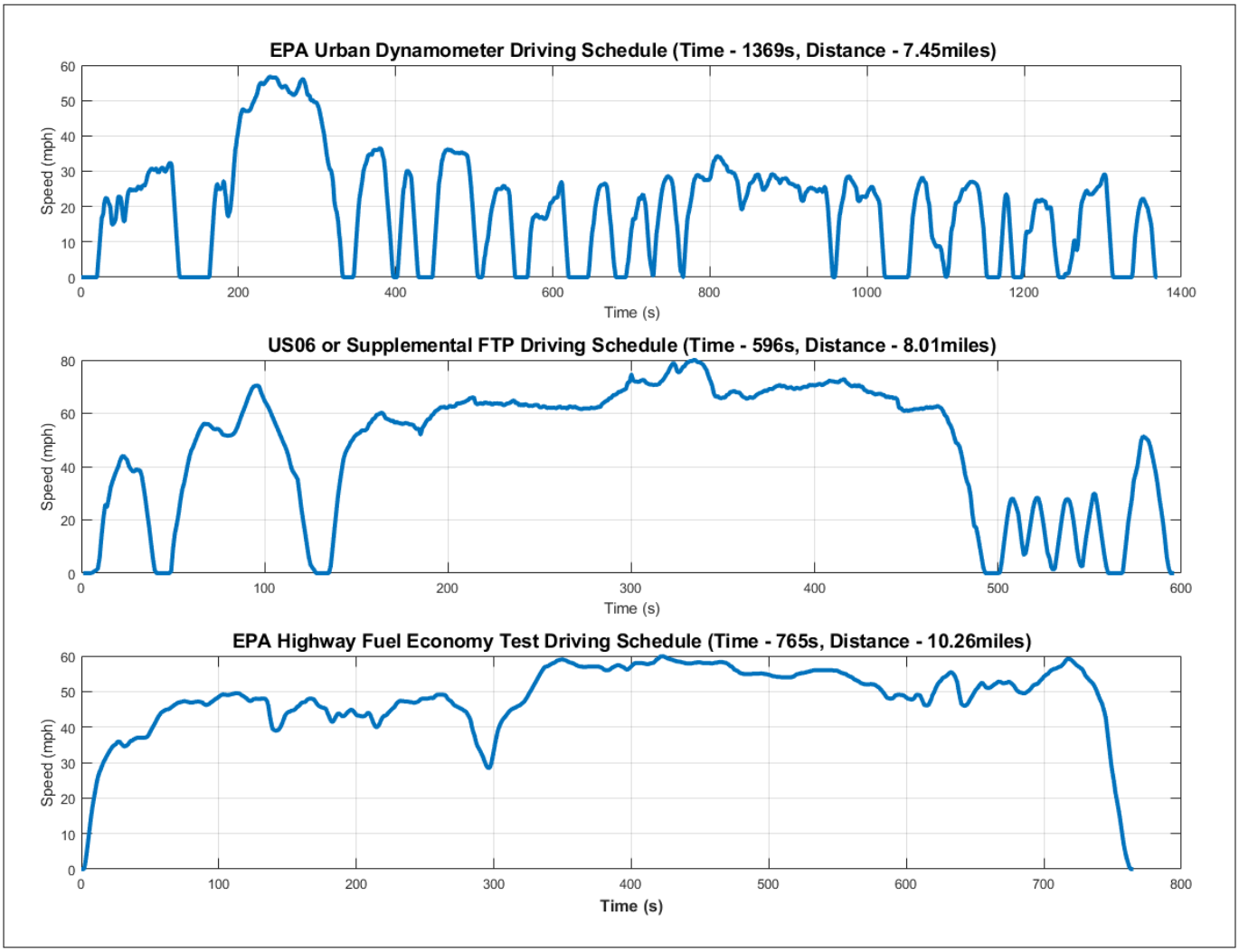

Figure 33 **Speed profile of EPA Drive Cycle for Light Passenger Vehicle. (Top) EPA Urban Dynamometer Driving Schedule (UDDS) Speed Profile, (Center) US06 Speed Profile, (Bottom) HWFET Speed Profile**

4.2 Thermal behavior

The EPA Urban Dynamometer Driving Schedule (UDDS) represents city driving conditions. It is used for light-duty vehicle testing. The speed profile is shown in Figure 33 (Top). The simulation results of UDDS are shown in the figure below.

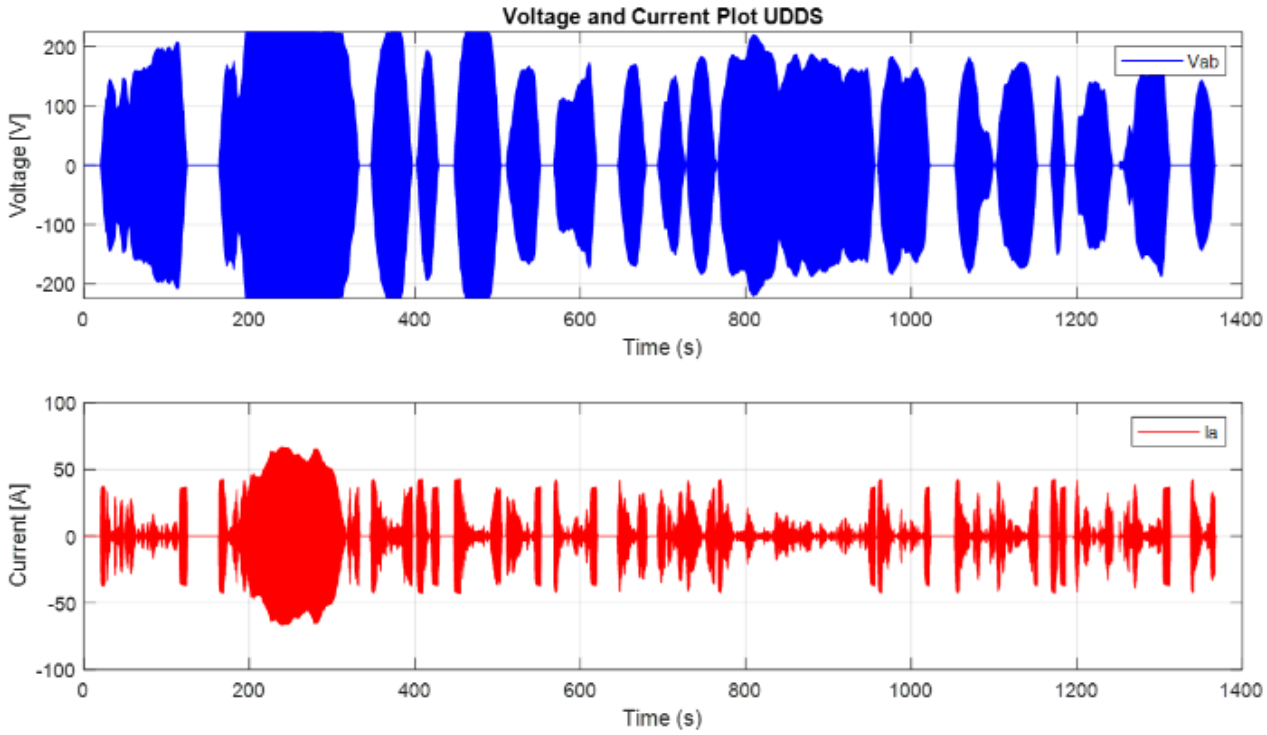

(a) Phase voltage and single device current plot

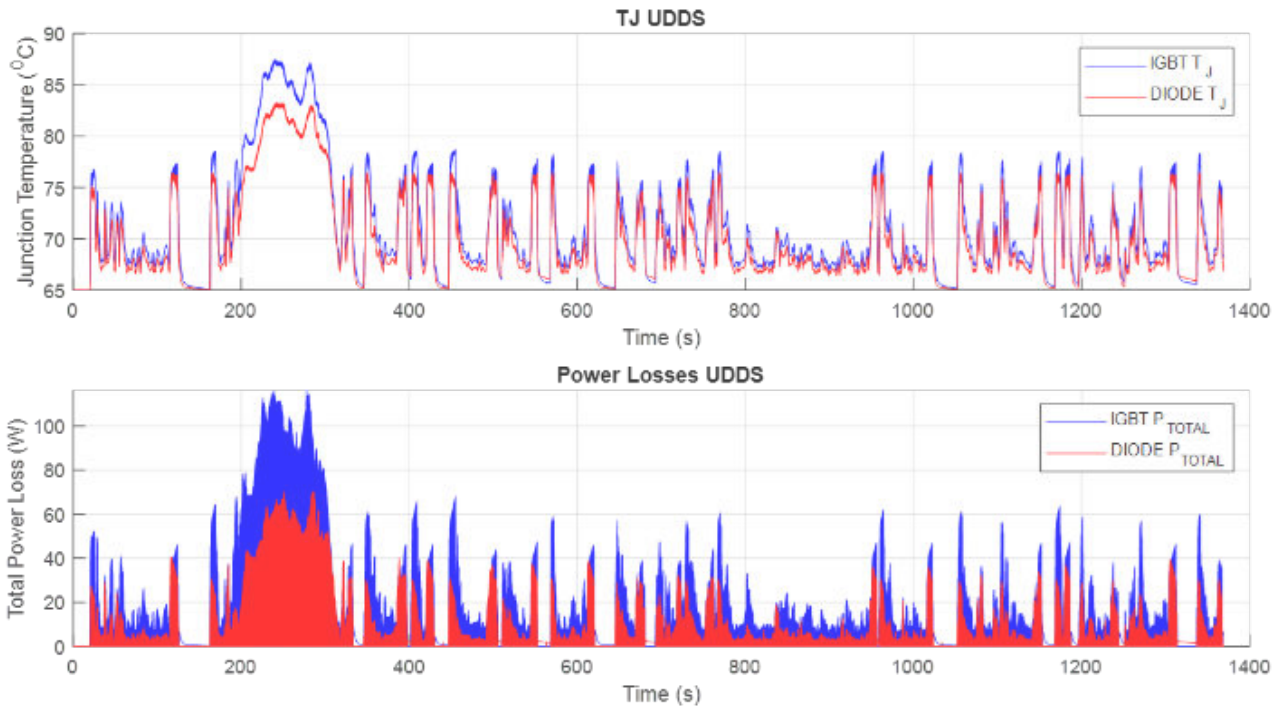

(b) Junction temperature and power losses

Figure 34 Simulation results of UDDS operation

Figure 34 (a) shows the phase-phase voltage and the single device current and Figure 34 (b) shows the junction temperature and instant power losses of IGBT and diode. DC BUS voltage is 450 V. The switching frequency

is 10 kHz. The coolant temperature is 65°C. The vehicle model and propulsion system are the same as WOT simulation in Application . Since UDDS is light-duty operating, the maximum device instant current is lower than 70 A. The maximum IGBT junction temperature is approximately 88°C.

The US06 is a high acceleration aggressive driving schedule that is often identified as the "Supplemental FTP" driving schedule. The speed profile is shown in Figure 33 (Center). DC BUS voltage is 450 V. The switching frequency is 10 kHz. The coolant temperature is 65°C. The vehicle model and propulsion system are the same as WOT simulation in Chapter 4.1. Figure 35 (a) shows the phase-phase voltage and single device current. Figure 35 (b) shows the junction temperature and the power losses. The maximum instant current is around 105 A. The maximum IGBT junction temperature is 101°C.

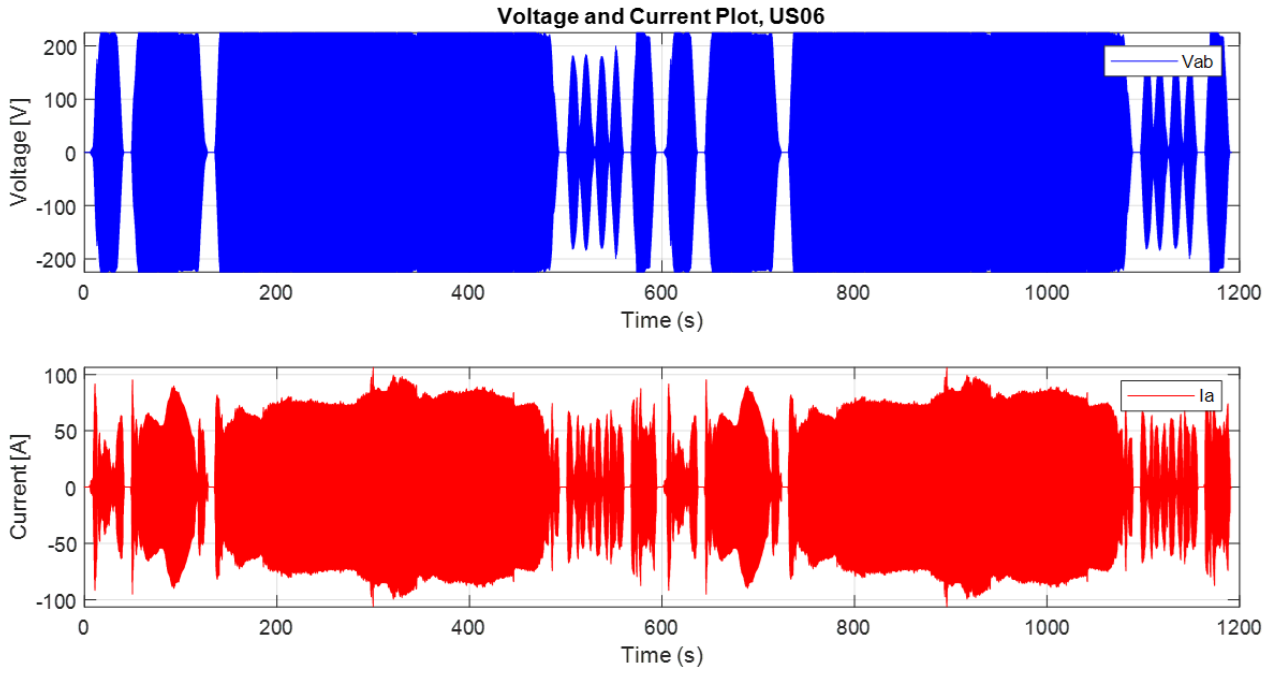

(a) Phase voltage and single device current plot

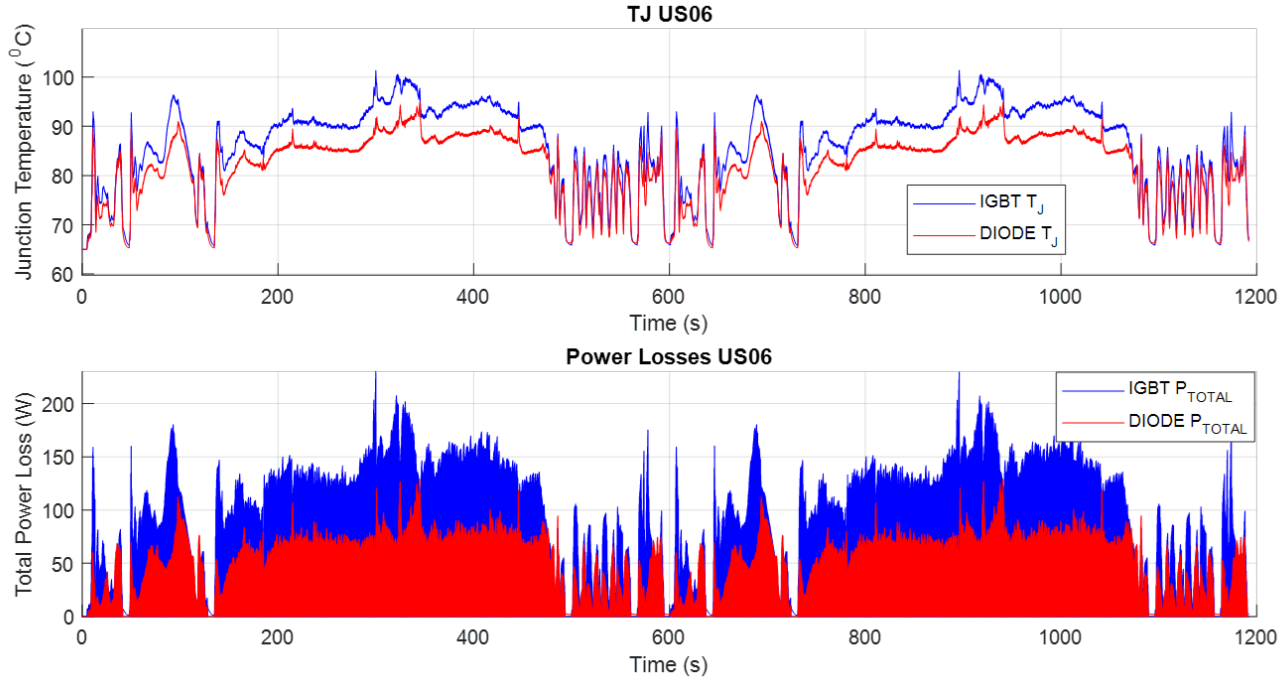

(b) Junction temperature and power losses

Figure 35 Simulation results of US06 operation

The Highway Fuel Economy Driving Schedule (HWFET) represents highway driving conditions under 60 mph. The speed profile is shown in Figure 33 (Bottom). DC BUS voltage is 450 V. The switching frequency is 10 kHz. The coolant temperature is 65°C. The vehicle model and propulsion system are the same as WOT simulation in Chapter 4.1. Figure 36 (a) shows the phase-phase voltage and single device current. Figure 36 (b) shows the

junction temperature and the power losses. The maximum instant current is around 70 A. The maximum IGBT junction temperature is 88°C.

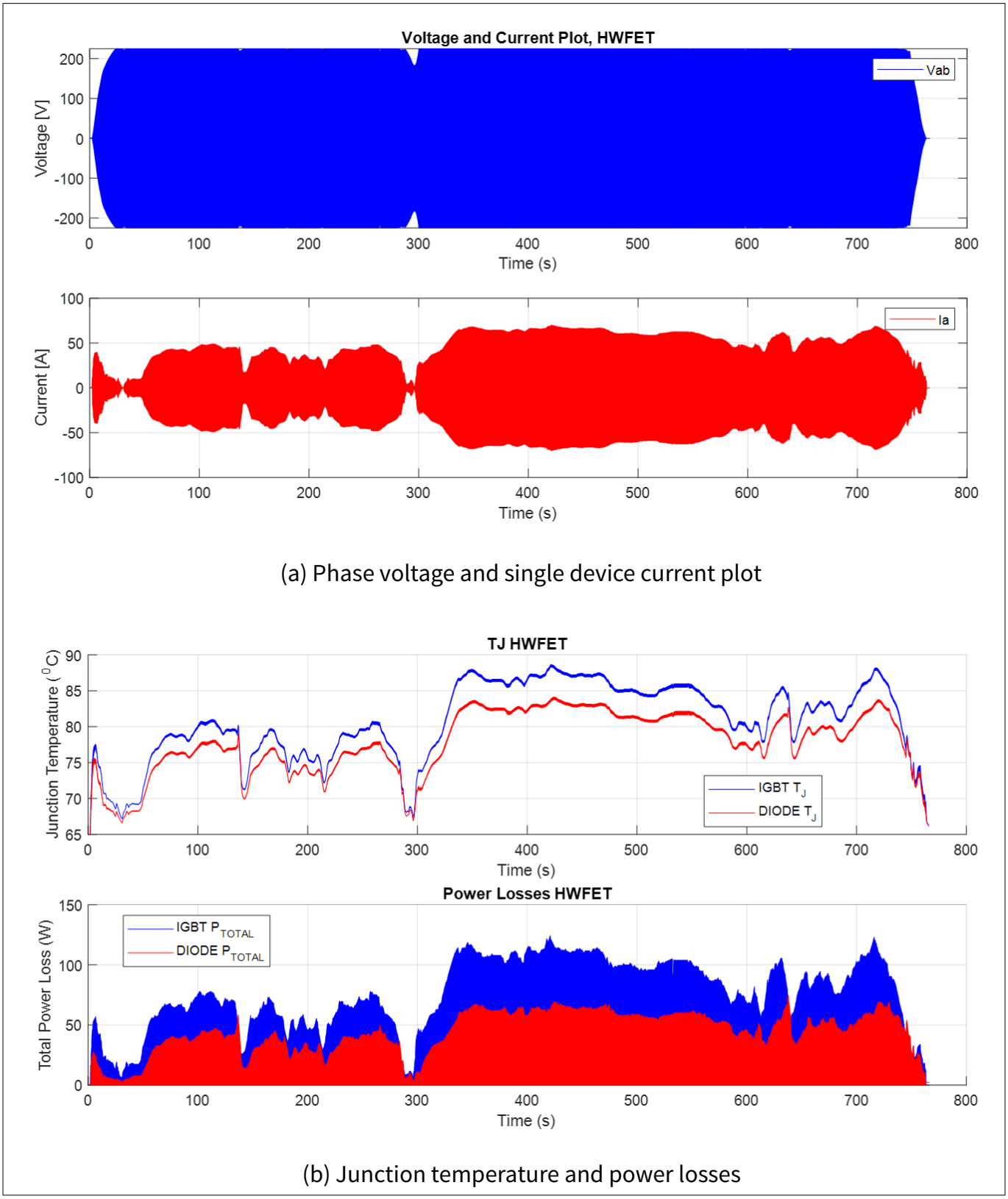

(a) Phase voltage and single device current plot

(b) Junction temperature and power losses

Figure 36 Simulation results of HWFET operation

4.3 EPA light vehicle power calculation

Performing rain flow-counting algorithm on the junction temperature curves to calculate the thermal cycles of these drive cycles above. With a proper Coffin-Manson coefficient, the converted equivalent thermal cycle of UDDS, US06, and HWFET at *delta-T* = 100°C are 0.03847, 0.13549, and 0.01511, respectively. With the profile is shown in Table 3 above, the equivalent thermal cycle at *delta-T* = 100°C of one-year usage of work, errand, and weekend/vacation are 83.5, 16.62, and 23.68, respectively. Therefore, the total thermal cycle at *delta-T* = 100°C is 123.80.

AIKQ200N75CP2 is qualified by the standard AEC-Q101, which requires that the thermal cycle at *delta-T* = 100°C of the device should be greater than 15000. Even though the thermal cycle capability of AIKQ200N75CP2 is much higher than 15000 cycles, in this application note, it is assumed that the minimum capability is 15000 cycles. Therefore, 10 years lifetime consumption is approximately 9.6%.

Note: For a deeper dive into the selection of Coffin-Manson coefficients and power cycling for discrete To-247 devices refer to [4]. In addition, as a base study, Infineon's IPOSIM online tool provides thermal simulation for this device. (https://iposim.infineon.com/). For more information on how to set up an Electrothermal simulation of high-power IGBTs in an inverter please refer to [5].

5 Gate drivers

There are several gate drivers from Infineon Technologies recommended for AIKQ200N75CP2 and AIKQ120N75CP2:

- 1EDI3020AS
- 1EDI3021AS
- 1EDI3023AS

The main features of these gate drivers are:

- 11.5 A peak current output
- DESAT protection
- OCP protection
- Active Miller Clamp
- Coreless transformer Isolation for IGBTs up to 1200 V

6 Qualification

Both the AIKQ200N75CP2 and AIKQ120N75CP2 are qualified according to AECQ101 [6]. Which is the industry standard “Stress test qualification for automotive-grade discrete semiconductors”. Nevertheless, Infineon quality goes far beyond and special quality requirements can be checked based on mission profiles can be evaluated upon special requested.

Currently, for module-based inverters, the AQG324 [7] qualification is a standard for many OEMs. If a module-like construction is created based on discrete devices, it is important to be aware of the differences between the AECQ101 and AQG324 Qualification. ECPE AQG324 is “Qualification of Power Modules for Use in Power Electronics Converter Units in Motor Vehicles” and AECQ101 focuses on discrete devices. Some of the common tests that differ are thermal-related stress tests like TST, Power Cycling, and Vibration testing among others.

In the case of AQG324 for the required tests, the whole power assembly has to be considered. All connections to the DC busbar, between power devices, and to the output terminals are therefore to be included in the test. Customers who need to fulfill this requirement test themselves the assembly.

References

[1] Infineon Technologies AG: *AN2017-1 TO-247PLUS Description of the packages and assembly guideline*; 81726 Munich, Germany: Infineon Technologies AG, 2017

[2] Infineon Technologies AG: *AN 2012-10 Electrical Safety and isolation in high voltage discrete component application and design hints*; 81726 Munich, Germany: Infineon Technologies AG, 2010

[3] M. H. Andreas Volke: *IGBT Modules. Technologies, Driver and Application, ISBN-10: 3000320768, ISBN-13: 978-3000320767*; Infineon Technologies, 2017

[4] G. Zeng, L. Borucki, O. Wenzel, O. Schilling and J. Lutz: *"First Results of Development of a Lifetime Model for Transfer Molded Discrete Power Devices," PCIM Europe 2018*; International Exhibition and Conference for Power Electronics, Intelligent Motion, Renewable Energy and Energy Management, 2018, pp. 1-8

[5] A. Kempitiya and W. Chou: *"Electro-thermal simulation for high power IGBTs for automotive applications," 2016 22nd International Workshop on Thermal Investigations of ICs and Systems (THERMINIC), 2016*; pp. 58-62, doi: 10.1109/THERMINIC.2016.7748648

[6] Automotive Electronics Council, Component Technical Committee: *AEC - Q101 STRESS TEST QUALIFICATION FOR AUTOMOTIVE GRADE DISCRETE SEMICONDUCTORS*

[7] ECPE: *AQG 324 Qualification of Power Modules for Use in Power Electronics Converter Units in Motor Vehicles , 03.1/2021 from 31 May, 2021*

Revision history

Document version	Date of release	Description of changes
V1.0	2022-01-11	Initial release

Trademarks

All referenced product or service names and trademarks are the property of their respective owners.

Edition 2022-01-11

Published by

Infineon Technologies AG

81726 Munich, Germany

Do you have a question about any aspect of this document?

Email: erratum@infineon.com

Document reference
IFX-krx1645527741790

Important notice

The information contained in this application note is given as a hint for the implementation of the product only and shall in no event be regarded as a description or warranty of a certain functionality, condition or quality of the product. Before implementation of the product, the recipient of this application note must verify any function and other technical information given herein in the real application. Infineon Technologies hereby disclaims any and all warranties and liabilities of any kind (including without limitation warranties of non-infringement of intellectual property rights of any third party) with respect to any and all information given in this application note.

The data contained in this document is exclusively intended for technically trained staff. It is the responsibility of customer's technical departments to evaluate the suitability of the product for the intended application and the completeness of the product information given in this document with respect to such application.

Warnings

Due to technical requirements products may contain dangerous substances. For information on the types in question please contact your nearest Infineon Technologies office.

Except as otherwise explicitly approved by Infineon Technologies in a written document signed by authorized representatives of Infineon Technologies, Infineon Technologies' products may not be used in any applications where a failure of the product or any consequences of the use thereof can reasonably be expected to result in personal injury.